Radiotherapy and Oncology 91 (2009) 433–437

Contents lists available at ScienceDirect

Radiotherapy and Oncology

journal homepage: www.thegreenjournal.com

Lung cancer RT

Relation between elective nodal failure and irradiated volume in non-small-cell lung cancer (NSCLC) treated with radiotherapy using conventional fields and doses

Naoko Sanuki-Fujimoto [a,*], Minako Sumi [a], Yoshinori Ito [a], Atsushi Imai [a], Yoshikazu Kagami [a], Ikuo Sekine [b], Hideo Kunitoh [b], Yuichiro Ohe [b], Tomohide Tamura [b], Hiroshi Ikeda [a]

[a] Department of Radiation Oncology, National Cancer Center Hospital, Japan
[b] Department of Thoracic Oncology and Internal Medicine, National Cancer Center Hospital, Japan

ARTICLE INFO

Article history:
Received 3 October 2008
Received in revised form 29 December 2008
Accepted 30 December 2008
Available online 21 January 2009

Keywords:
Chemoradiotherapy
Elective nodal failure
Elective nodal irradiation
Non-small-cell lung carcinoma
Radiotherapy

ABSTRACT

Introduction: The role of elective nodal irradiation of non-small-cell lung cancer (NSCLC) patients treated with radiotherapy remains unclear. We investigated the significance of treating clinically uninvolved lymph nodes by retrospectively analyzing the relationship between loco-regional failure and the irradiated volume.

Methods: Between 1998 and 2003, patients with IA–IIIB NSCLC were treated with radiotherapy. The eligibility criteria for this study were an irradiation dose of 60 Gy or more and a clinical response better than stable disease. Typical radiotherapy consisted of 40 Gy/20 fr to the tumor volumes (clinical target volume of the primary tumor [CTVp], of the metastatic lymph nodes [CTVn], and of the subclinical nodal region [CTVs]), followed by off-cord boost to CTVp+n to a total dose 60–68 Gy/30–34 fr. The relationship between the sites of recurrence and irradiated volumes was analyzed.

Results: A total of 127 patients fulfilled the eligibility criteria. Their median overall and progression-free survival times were 23.5 (range, 4.2–109.7) and 9.0 months (2.2–109.7), respectively. At a median follow-up time of 50.5 months (range, 14.2–83.0) for the surviving patients, the first treatment failure was observed in 95 patients (loco-regional; 41, distant; 42, both; 12). Among the patients with loco-regional failure, in-field recurrence occurred in 38 patients, and four CTVs recurrences associated with CTVp+n failure were observed. No isolated recurrence in CTVs was observed.

Conclusions: In-field loco-regional failure, as well as distant metastasis, was a major type of failure, and there was no isolated elective nodal failure. Radiation volume adequacy did not seem to affect elective nodal failure.

© 2009 Elsevier Ireland Ltd. All rights reserved. Radiotherapy and Oncology 91 (2009) 433–437

Radiation therapy is an integral component of the multi-modal treatment of non-small-cell lung cancer (NSCLC). Recent phase III studies have demonstrated that concomitant chemoradiotherapy improves survival, and this has resulted in the general acceptance of concurrent chemoradiotherapy as one of the standard treatments for locally advanced NSCLC [1]. Despite the improved survival, however, most patients die from their disease as a result of local or distant failure.

Local failure remains a major challenge when treating NSCLC with radiotherapy. A number of studies of dose escalation to the gross tumor volume (GTV) have been conducted as a means of improving local control [2–5]. The conventional radiation fields for NSCLC typically encompass the entire mediastinum and ipsilateral hilum (elective nodal region) to deliver a dose of 40 Gy, even without evidence of disease in these areas, followed by a 20 Gy boost to the GTV. However, the conventional treatment has added considerable morbidity and can limit the dose escalation. In phase I–II dose escalation studies, there is a trend toward omitting the practice of elective nodal irradiation (ENI) after their experiences with toxicity, which is not based on direct evidence [2–5]. According to those studies, omitting ENI has not sacrificed treatment outcomes so far. They also analyzed patterns of recurrence in relation to irradiated volume in a dose escalation setting [6].

By contrast, the current literature provides limited information regarding patterns of failure when conventional fields and doses are used [7,8]. Since it is important to know whether loco-regional failure is within or outside the irradiation field, we retrospectively analyzed patterns of failure after radiation therapy for NSCLC, especially in regard to the relationship between local failure and irradiated volume.

Methods and materials

Patients

Between January 1998 and March 2003, 263 patients with newly diagnosed NSCLC were treated with thoracic radiation therapy,

* Corresponding author. Address: Department of Radiation Oncology, National Cancer Center Hospital, 1-1, Tsukiji 5-chome, Chuo-ku, Tokyo 104-0045, Japan.
E-mail address: nao5-tky@umin.ac.jp (N. Sanuki-Fujimoto).

0167-8140/$ - see front matter © 2009 Elsevier Ireland Ltd. All rights reserved.
doi:10.1016/j.radonc.2008.12.013

with or without chemotherapy, at the National Cancer Center Hospital. All tumors were cytologically or histologically confirmed NSCLC. Patients' disease was staged by the tumor-node-metastasis (TNM) staging system (UICC, version 6, 2002). The diagnostic workup included a bone scan, brain scan by computed tomography (CT) or magnetic resonance imaging, CT scan of the chest, and CT or ultrasound imaging of the abdomen. The criteria for inclusion in this study were irradiation with a dose of 60 Gy or more as a part of the initial treatment and a clinical response better than stable disease. After excluding patients with metastatic disease, whose primary tumor was located in the apex of the lung (superior sulcus), and whose post-treatment evaluation was inadequate, the remaining 127 patients served as the subjects of the analysis.

Details of treatment

Radiotherapy

Gross tumor volume (GTV) was defined as the demonstrable extent of the primary tumor and the metastatic lymph nodes, GTVp and GTVn, respectively. GTVn was defined as abnormally enlarged regional lymph nodes measuring over 1.0 cm along their short axis. Clinical target volume (CTV) consisted of the adjacent mediastinum and ipsilateral hilum (CTV of the subclinical nodal region, CTVs) as well as CTVp and CTVn which were assumed to be equal to GTVp and GTVn, respectively. A planning target volume (PTV) margin of 1–1.5 cm was drawn around each CTV.

External-beam radiotherapy with a 6, 10, or 15 MV photon beam was delivered using a linear accelerator. A majority of the patients were treated with anteroposterior opposing fields encompassing CTV to a dose of 40 Gy/20 fractions (2 Gy per fraction, 5 days per week), followed by an off-cord boost to the GTV by oblique opposing fields, to a total dose of 60–68 Gy/30–34 fractions. No attempt was made to encompass the supraclavicular areas in most patients; the supraclavicular areas were treated only electively. Initially, treatment planning was performed by using an X-ray simulator for the anteroposterior fields and a CT-port for the oblique opposing fields, but after the end of 1999, most treatment planning, especially to define the off-cord boost, was performed using a CT-based planning system (FOCUS, Computed Medical Systems).

The dose to the spinal cord was limited to 45–50 Gy. The size of the treatment fields was adjusted so that it did not exceed half of the hemithorax before introducing CT-based planning system, or so that the volume of normal lung tissue receiving a dose over 20 Gy would be less than 40%.

Chemotherapy

Systemic chemotherapy was used in 87 patients (68.5%), and the majority of the patients received platinum-based chemotherapy sequentially or concurrently with the radiation therapy. One of the representative regimens was 2–3 cycles of cisplatin 80 mg/sqm on day 1 and vinorelbine 25 mg/sqm on days 1 and 8 (or vindesine 3 mg/sqm on days 1, 8, and 15) in 21–28 days. The second most common regimen was cisplatin 80 mg/sqm on day 1, vindesine 3 mg/sqm on days 1 and 8, and mitomycin C 8 mg/sqm on day 1, in 21–28 days. The other regimens are summarized in Table 1.

Evaluation

Patients were followed at 4- to 6-week intervals for 6 months after treatment and at 3- to 6-month intervals thereafter. Chest X-ray and laboratory workups were performed at each post-treatment visit. Unless there were changes in the chest X-ray or in symptoms, a CT scan was performed about 2–3 months after the treatment for the assessment of the treatment response, and every 6–12 months thereafter. Follow-up information was obtained from the medical charts and death certificates.

Table 1
Baseline patient characteristics.

Characteristics	Patients	(%)
Median age (yr)	65 (36–83)	
Gender		
Male	106	83
Female	21	17
Performance status (WHO)		
0	12	9
1	109	86
2	6	5
Stage		
I (A/B)	5(1/4)	4
II (A/B)	12(3/9)	9
III (A/B)	110(59/51)	87
Histology		
Adenocarcinoma	64	50
Squamous cell carcinoma	39	31
Large cell carcinoma	4	3
NSCLC (not otherwise specified)	20	16
Chemotherapy (concurrent/sequential)	87(63/24)	69
Chemotherapy regimens		
Cisplatin + vindesine or vinorelbine	48	55
Carboplatin + paclitaxel	12	14
MVP (cisplatin + vindesine + mitomycin)	12	14
Nedaplatin or nedaplatin + paclitaxel	11	13
Others	4	5

When evaluating overall survival, an event was defined as death from any cause. When evaluating progression-free survival, an event was defined as documented tumor progression (loco-regional or distant) or death from any cause. Local or loco-regional failure was judged to have occurred if there was radiographic evidence of progressive disease. Absence of progression of residual disease for more than 6 months following treatment was considered evidence of loco-regional control. A recurrence in supraclavicular nodes was considered regional failure, not an elective nodal failure, because the supraclavicular regions are not routinely included within the radiation fields in our practice. Treatment failure was not always confirmed histologically. Elective nodal failure (ENF) was defined as recurrence in CTVs without evidence of local failure, as the first event or even after distant metastasis.

The adequacy of field borders was assessed in terms of CTVs coverage and PTV margin in patients with loco-regional failure. The failure patterns were analyzed to distinguish in-field recurrence from out-of-field recurrence; "in-field" included CTVs as well as CTVp and CTVn.

The Kaplan–Meier method was used from the start of the treatment to calculate the overall survival and progression-free survival of all the 127 patients.

Results

A total of 127 patients, median age 65 years (range, 36–83), met the criteria for evaluation in this study. The majority of patients had stage IIIA ($n = 59$) or IIIB ($n = 51$) disease. Other baseline characteristics of the patients and details of their treatment are summarized in Table 1.

At a median follow-up time of 50.5 months (range, 14.2–83.0) of the surviving patients, 95 had experienced treatment failure. Median survival time was 23.5 months (range, 4.2–109.7), and median time to progression was 9.0 months (range, 2.2–109.7). The 2-year cumulative survival rate and 2-year progression-free survival rate were 51.4% and 27.6%, respectively. The survival

curves are shown in Fig. 1. Patients with early progressions were excluded because of the criteria for inclusion in this study: a clinical response better than stable disease.

Eighty-seven (69%) patients received chemotherapy concomitantly or sequentially with the radiotherapy. The overall survival time of the patients who received chemotherapy was 21.7 months (range, 7.6–33.9), as opposed to 19.1 months (range, 6.8–32.7) among those who did not receive chemotherapy, and the difference was not statistically significant ($p = 0.10$). There were no statistically significant differences in disease-free survival nor loco-regional control according to whether the patients had received chemotherapy. Concurrent use of chemoradiotherapy did not affect survival among the 87 patients who received chemotherapy (data not shown).

There were 53 patients with a first loco-regional failure, alone ($n = 41$) or with distant metastasis ($n = 12$), and the majority of the failures were in-field ($n = 38$, 72%). Nine (21%) patients had out-of-field recurrences in the form of supraclavicular node metastasis ($n = 5$) or pleural metastasis ($n = 4$), with or without local recurrence. There were no isolated ENFs (Table 2).

Four patients (7%) experienced nodal failure in CTVs simultaneously with local or distant failure. Three of them had received a prophylactic dose of 40 Gy to the CTVs, and the other had inadequate margin of the CTVs field. Other characteristics of these patients are shown in Table 3. There were no "marginal only" failures among in-field failures; all the failures at the field borders were associated with out-of-field failures.

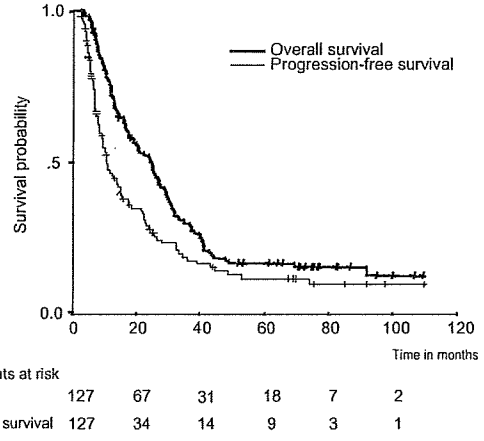

Fig. 1. Overall and progression-free survival curves of all the 127 patients. Patients with early progressions were excluded because of the criteria for inclusion in this study: a clinical response better than stable disease.

Table 2
Details of all the first failures.

Types of event	Patients	%
Loco-regional alone	41	43%
In-field		
CTVpn	30	
CTVpn + CTVs[a]	2	
In-field + out-of-field		
CTVpn + pleural effusion	2	
CTVpn + supraclavicular nodes	2	
Out-of-field		
Supraclavicular nodes	3	
Pleural effusion[b]	2	
Loco-regional + distant	12	13%
In-field + out-of-field		
CTVpn + CTVs	2	
Distant alone	42	44%
All events	95	

[a] One also had concurrent failure in the contralateral hilum.
[b] One also had concurrent supraclavicular recurrence.

Conventional X-ray simulation was performed in 8 (6%) patients, while 70 (55%) had CT-based simulation and remaining 49 (39%) had both (initially with X-ray simulation, followed by CT-based simulation for off-cord boost). A majority ($n = 122$, 96%) of the patients were treated with anteroposterior opposing fields as elective nodal irradiation, followed by oblique opposing fields to the total dose.

ENI was incomplete ($n = 12$) or not performed ($n = 6$) in 18 of the 53 patients with loco-regional failure because of diminished pulmonary function or deteriorated performance status. All the incomplete ENIs were due to insufficient CTVs coverage. In 12 of the 18 patients, the failure was in the tumor volume, in 3 patients it was in the pleura, and in 2 patients it was in the supraclavicular nodes. Only 1 patient had recurrence in both the tumor volume and the uninvolved nodal area.

Discussion

In this series of NSCLC cases treated with conventional fields and doses, the loco-regional failures after radiotherapy mainly occurred in the tumor volumes, and there were no isolated ENFs.

There are several possible reasons for these results. First, micrometastasis in the CTVs may have been controlled by prophylactic delivery of 40 Gy to the region, and depending on the location of the primary tumor, the sites of occult metastasis may often have received additional unintentional radiation doses. Kepka et al. reported an isolated ENF rate of 9% in 185 patients treated with the ENI using 3-dimensional conformal radiotherapy (3D-CRT). Their analysis showed that the ENF occurred more frequently in the regions that received under 40 Gy than in the regions that received higher doses (69% vs. 31%, respectively, $p = 0.04$) [7]. However, despite the same ENF rate of 9% in 1705 patients in the four trials conducted by the Radiation Therapy Oncology Group (RTOG), a retrospective evaluation of in-field progression revealed that neither in-field progression nor survival was affected by the adequacy of ENI [8]. Field adequacy did not have any negative impact on regional control in our series either (Tables 3).

Second, the amount of micrometastasis in unenlarged mediastinal regional nodes may have been small enough to be controlled by chemotherapy, which has been shown to have activity that reduces the incidence of distant micrometastasis in advanced NSCLC. However, the degree of systemic and local efficacy of chemotherapy did not reach statistical significance in our series, probably because of the small number of patients and their heterogeneity (data not shown).

Third, since the failure sites in the majority of patients were distant, they would have died of their disease before the ENF became apparent. As a result, the loco-regional failure rates may have been lower than their true values because we did not investigate regional sites once a patient developed distant metastasis.

The therapeutic significance of treating subclinical nodal regions during and after surgery for NSCLC has been questioned. Some studies have established the presence of considerable microscopic nodal disease in clinically uninvolved lymph nodes [9,10], but the role of mediastinal lymphadenectomy remains controversial and has been limited to the precise staging of the disease [11–13]. A study by Izbicki et al. which compared systemic mediastinal lymphadenectomy with mediastinal lymph node sampling showed that radical systemic mediastinal lymphadenectomy had no effect on the disease-free or overall survival of patients with limited nodal involvement [13,14]. The role of adjuvant radiotherapy after complete resection also remains unclear [15–17]. A systemic

Table 3
Patients with CTVs failure.

	Patient #1	Patient #2	Patient #3	Patient #4
Age (yr)/Sex	45/Female	74/Female	61/Male	78/Male
Reason for inoperability	Unresectable	Unresectable	Decreased pulmonary function	Unresectable, age
Stage	IIIA	IIIA	IIB	IIIB
Primary location	Left lower lobe	Right upper lobe	Right lower lobe	Left upper lobe
Histology	Adenocarcinoma	Adenocarcinoma	Squamous cell carcinoma	Adenocarcinoma
Chemotherapy	Yes	Yes	No	No
Response	Partial response	Partial response	Partial response	Partial response
Site of first failure	Distant and loco-regional	Distant and loco-regional	Loco-regional	Loco-regional
Field border adequacy	Yes	Yes	No	Yes
Dose to CTVs failure	40	40	0	40
Death	No	No	Yes	No

review and meta-analysis [18] showed that postoperative radiotherapy was detrimental to patients with early NSCLC, although there may have been some efficacy in patients with N2 tumors. These arguments also raise questions about the clear benefit of ENI in regard to survival.

In-field loco-regional failure was a major site of failure in the current study: all the recurrences in the CTVs were associated with failure in the gross tumor volume. Thus, more intensive treatment strategies are needed to enhance loco-regional control without sacrificing safety. One possible strategy is to reduce the ENI field in regard to the patients' risk factors while escalating the total dose. Such an attempt has already been made in regard to surgery: Asamura et al. retrospectively reviewed the prevalence of lymph node metastasis with respect to the location of the primary tumor or other characteristics to decide on the optimal lobe-specific extent of systematic lymph node dissection for NSCLC [19,20]. By using such predictors, including the location of the primary tumor, histology, or nodal stage [21–24], it is possible to identify the nodal areas at risk and to optimize the extent of ENI in radiation therapy as well. On the other hand, more precise diagnosis by novel technology, such as positron emission tomography [25], may enable the omission of ENI and avoid unnecessary irradiation to areas at low risk for subclinical disease.

In terms of the technical feasibility of dose escalation, Grills et al. found that intensity-modulated radiation therapy without ENI for NSCLC increased the deliverable mean target dose in node-positive patients by 25–30% over 3D-CRT and by 130–140% over traditional ENI [26].

Because omitting ENI is likely to leave microscopic disease untreated, there is concern that it may result in increased failure in these areas. However, the preliminary results of dose escalation trials have shown that isolated ENF outside the irradiated volume occurred in fewer than 6% of the cases and that omission of ENI did not seem to sacrifice outcome [2–5,27]. There is insufficient evidence to support the use of ENI for any patient with localized NSCLC (Stages I–III), irrespective of whether chemotherapy is administered [28]. There has been only one randomized trial that compared high-dose thoracic radiotherapy without ENI and standard dose radiotherapy with ENI, and it showed a survival benefit of high-dose thoracic radiotherapy without ENI [29]. One possible explanation for this finding is that incidental doses to elective nodal areas may contribute to the eradication of the subclinical disease. The pattern of ENF according to nodal regions was described by Rosenzweig et al., who implemented the use of involved-field radiation therapy with dose escalation in 524 patients [6]. Since the majority of the 42 ENFs that were observed occurred in the areas that received less than 45 Gy, the incidental doses to elective nodal areas may have been substantial despite the attempt not to treat these regions in their study. In addition, Zhao et al. reported that involved-field radiation therapy with a dose escalated to 70 Gy delivered a considerable dose to CTVs, and when the primary tumor was large or centrally located, the percentages of CTVs in the lower paratracheal region, subcarinal region and ipsilateral hilar region receiving over 40 Gy were 33%, 39%, and 98%, respectively [30].

Because of the retrospective nature of our study, no conclusions about the value of ENI for NSCLC can be drawn. However, the finding that in-field loco-regional failure, as well as distant metastasis, was a major type of failure with the standard field and dose of thoracic radiotherapy confirmed the need for more intensive treatment.

Further investigation to verify the true significance of ENI or to identify best candidates for ENI is necessary before it is abandoned in the context of dose escalation.

Conclusion

The loco-regional failures after radiotherapy in this series of NSCLC cases treated with conventional fields and doses mainly occurred in the tumor volumes, and there were no isolated ENFs. The results confirmed the need for more intense treatment to improve local control.

References

[1] Penland SK, Socinski MA. Management of unresectable stage III non-small cell lung cancer: the role of combined chemoradiation. Semin Radiat Oncol 2004;14:326–34.
[2] Belderbos JS, De Jaeger K, Heemsbergen WD, et al. First results of a phase I/II dose escalation trial in non-small cell lung cancer using three-dimensional conformal radiotherapy. Radiother Oncol 2003;66:119–26.
[3] Rosenman JG, Halle JS, Socinski MA, et al. High-dose conformal radiotherapy for treatment of stage IIIA/IIIB non-small-cell lung cancer: technical issues and results of a phase I/II trial. Int J Radiat Oncol Biol Phys 2002;54:348–56.
[4] Socinski MA, Morris DE, Halle JS, et al. Induction and concurrent chemotherapy with high-dose thoracic conformal radiation therapy in unresectable stage IIIA and IIIB non-small-cell lung cancer: a dose-escalation phase I trial. J Clin Oncol 2004;22:4341–50.
[5] Wu KL, Jiang GL, Liao Y, et al. Three-dimensional conformal radiation therapy for non-small-cell lung cancer: a phase I/II dose escalation clinical trial. Int J Radiat Oncol Biol Phys 2003;57:1336–44.
[6] Rosenzweig KE, Sura S, Jackson A, et al. Involved-field radiation therapy for inoperable non small-cell lung cancer. J Clin Oncol 2007;25:5557–61.
[7] Kepka A, Szajda SD, Jankowska A, et al. Risk of isolated nodal failure for non-small cell lung cancer (NSCLC) treated with the elective nodal irradiation (ENI) using 3D-conformal radiotherapy (3D-CRT) techniques – A retrospective analysis. Acta Oncol 2008;47:95–103.
[8] Emami B, Mirkovic N, Scott C, et al. The impact of regional nodal radiotherapy (dose/volume) on regional progression and survival in unresectable non-small cell lung cancer: an analysis of RTOG data. Lung Cancer 2003;41:207–14.
[9] Izbicki JR, Passlick B, Hosch SB, et al. Mode of spread in the early phase of lymphatic metastasis in non-small-cell lung cancer: significance of nodal micrometastasis. J Thorac Cardiovasc Surg 1996;112:623–30.
[10] Oda M, Watanabe Y, Shimizu J, et al. Extent of mediastinal node metastasis in clinical stage I non-small-cell lung cancer: the role of systematic nodal dissection. Lung cancer 1998;22:23–30.
[11] Keller SM, Adak S, Wagner H, et al. Mediastinal lymph node dissection improves survival in patients with stages II and IIIa non-small cell lung cancer. Eastern Cooperative Oncology Group. Ann Thorac Surg 2000;70:358–65 [discussion 365–366].
[12] Sugi K, Nawata K, Fujita N, et al. Systematic lymph node dissection for clinically diagnosed peripheral non-small-cell lung cancer less than 2 cm in diameter. World J Surg 1998;22:290–4 [discussion 294–295].

[13] Izbicki JR, Passlick B, Pantel K, et al. Effectiveness of radical systematic mediastinal lymphadenectomy in patients with resectable non-small cell lung cancer: results of a prospective randomized trial. Ann Surg 1998;227:138–44.
[14] Izbicki JR, Thetter O, Habekost M, et al. Radical systematic mediastinal lymphadenectomy in non-small cell lung cancer: a randomized controlled trial. Br J Surg 1994;81:229–35.
[15] Dautzenberg B, Arriagada R, Chammard AB, et al. A controlled study of postoperative radiotherapy for patients with completely resected non-small cell lung carcinoma. Groupe d'Etude et de Traitement des Cancers Bronchiques. Cancer 1999;86:265–73.
[16] Keller SM, Adak S, Wagner H, et al. A randomized trial of postoperative adjuvant therapy in patients with completely resected stage II or IIIA non-small-cell lung cancer. Eastern Cooperative Oncology Group. N Engl J Med 2000;343:1217–22.
[17] Trodella L, Granone P, Valente S, et al. Adjuvant radiotherapy in non-small cell lung cancer with pathological stage I: definitive results of a phase III randomized trial. Radiother Oncol 2002;62:11–9.
[18] Rowell NP. Postoperative radiotherapy in non-small-cell lung cancer. Lancet 1998;352:1384 [author reply 1385–1386].
[19] Asamura H, Nakayama H, Kondo H, et al. Lobe-specific extent of systematic lymph node dissection for non-small cell lung carcinomas according to a retrospective study of metastasis and prognosis. J Thorac Cardiovasc Surg 1999;117:1102–11.
[20] Asamura H, Nakayama P, Kondo H, et al. Lymph node involvement, recurrence, and prognosis in resected small, peripheral, non-small-cell lung carcinomas: are these carcinomas candidates for video-assisted lobectomy? J Thorac Cardiovasc Surg 1996;111:1125–34.
[21] Komaki R, Scott CB, Bynandt R, et al. Failure patterns by prognostic group determined by recursive partitioning analysis (RPA) of 1547 patients on four radiation therapy oncology group (RTOG) studies in inoperable nonsmall-cell lung cancer (NSCLC). Int J Radiat Oncol Biol Phys 1998;42:263–7.
[22] Komaki R, Scott CB, Sause WT, et al. Induction cisplatin/vinblastine and irradiation vs. irradiation in unresectable squamous cell lung cancer: failure patterns by cell type in RTOG 88-08/ECOG 4588. Radiation Therapy Oncology Group. Eastern Cooperative Oncology Group. Int J Radiat Oncol Biol Phys 1997;39:537–44.
[23] Movsas B, Scott C, Sause W, et al. The benefit of treatment intensification is age and histology-dependent in patients with locally advanced non-small cell lung cancer (NSCLC): a quality-adjusted survival analysis of radiation therapy oncology group (RTOG) chemoradiation studies. Int J Radiat Oncol Biol Phys 1999;45:1143–9.
[24] Suzuki K, Nagai K, Yoshida J, et al. Clinical predictors of N2 disease in the setting of a negative computed tomographic scan in patients with lung cancer. J Thorac Cardiovasc Surg 1999;117:593–8.
[25] Vansteenkiste J, Fischer BM, Booms C, et al. Positron-emission tomography in prognostic and therapeutic assessment of lung cancer: systematic review. Lancet Oncol 2004;5:531–40.
[26] Grills IS, Yan D, Martinez AA, et al. Potential for reduced toxicity and dose escalation in the treatment of inoperable non-small-cell lung cancer: a comparison of intensity-modulated radiation therapy (IMRT), 3D conformal radiation, and elective nodal irradiation. Int J Radiat Oncol Biol Phys 2003;57:875–90.
[27] Senan S, Burgers S, Samson MJ, et al. Can elective nodal irradiation be omitted in stage III non-small-cell lung cancer? Analysis of recurrences in a phase II study of induction chemotherapy and involved-field radiotherapy. Int J Radiat Oncol Biol Phys 2002;54:999–1006.
[28] Senan S, De Ruysscher D, Girard P, et al. Literature-based recommendations for treatment planning and execution in high-dose radiotherapy for lung cancer. Radiother Oncol 2004;71:139–46.
[29] Yuan S, Sun X, Lim L, et al. A randomized study of involved-field irradiation versus elective nodal irradiation in combination with concurrent chemotherapy for inoperable stage III nonsmall cell lung cancer. Am J Clin Oncol 2007;30:239–44.
[30] Zhao L, Chen M, Ten Haken R, et al. Three-dimensional conformal radiation may deliver considerable dose of incidental nodal irradiation in patients with early stage node-negative non-small cell lung cancer when the tumor is large and centrally located. Radiother Oncol 2007;82:153–9.

Circulating Endothelial Cells in Non-small Cell Lung Cancer Patients Treated with Carboplatin and Paclitaxel

Makoto Kawaishi, MD, Yutaka Fujiwara, MD,† Tomoya Fukui, MD,* Terufumi Kato, MD,* Kazuhiko Yamada, MD,† Yuichiro Ohe, MD, PhD,† Hideo Kunitoh, MD, PhD,† Ikuo Sekine, MD, PhD,† Noboru Yamamoto, MD, PhD,† Hiroshi Nokihara, MD, PhD,† Takeshi Watabe, PhD,‡ Yuji Shimoda, PhD,‡ Tokuzo Arao, MD, PhD,§ Kazuto Nishio, MD, PhD,§ Tomohide Tamura, MD† and Fumiaki Koizumi, MD, PhD**

Introduction: Circulating endothelial cells (CECs) increase in cancer patients and play an important role in tumor neovascularization.
Methods: This study was designed to investigate the role of CEC as a marker for predicting the effectiveness of a carboplatin plus paclitaxel based first line chemotherapy in advanced non-small cell lung cancer (NSCLC).
Results: The CEC count in 4 ml of peripheral blood before starting chemotherapy (baseline value) was significantly higher in NSCLC patients, ranging from 32 to 4501/4 ml (n = 31, mean ± SD = 595 ± 832), than in healthy volunteers (n = 53, 46.2 ± 86.3). We did not detect a significant correlation between the CEC count and estimated tumor volume. CECs were significantly decreased by chemotherapy as compared with pretreatment values (175.6 ± 24 and 173.0 ± 24, day +8, +22, respectively). We investigated the correlation between baseline CEC and the clinical effectiveness of chemotherapy. CEC values are significantly higher in patients with clinical benefit (partial response and stable disease, 516 ± 458, 870.8 ± 1215, respectively) than in progressive disease patients (211 ± 150). Furthermore, a statistically significant decrease in CECs, on day 22, was observed only in patients with partial response. Patients who had a baseline CEC count greater than 400/4 ml showed a longer progression-free survival (>400, 271 days [range: 181–361] versus <400, 34 [range: 81–186], p = 0.019).
Conclusion: CEC is suggested to be a promising predictive marker of the clinical efficacy of the CBDCA plus paclitaxel regimen in patients with NSCLC.

Key Words: Circulating endothelial cell, NSCLC, Chemotherapy.

(*J Thorac Oncol.* 2009;4: 208–213)

Angiogenesis plays a critical role in the growth and metastasis of solid tumors.[1] The clinical importance of angiogenesis in human tumors has been demonstrated by several reports indicating a positive relationship between the blood vessel density in the tumor mass and poor prognosis, i.e., survival, in patients with various types of cancers including non-small cell lung cancer (NSCLC).[2–6] Furthermore, Natsume et al.[7] reported the antitumor activities of anticancer agents to be less active against vascular endothelial growth factor-secreting cells (SBC-3/VEGF), in vivo as compared with its mock transfectant (SBC-3/Neo). In recent years, antiangiogenic agents have also been demonstrated to be active against a variety of malignancies, including lung, colorectal, and renal cancer.[8–10] Thus, angiogenesis is a promising target for cancer treatment and is related to the prognosis and efficacy of these drugs, though the tumor vessel biomarkers which predict the effectiveness of antiangiogenic agents and other anticancer agents are not always useful and have not become well-established.

Circulating endothelial cells (CECs) have been recognized as a useful biomarker for vascular damage. CECs are increased in cardiovascular disease, vasculitis, infectious disease, and various cancers.[11–14] Recently, CECs were found to be more numerous and viable in cancer patients than in healthy subjects.[14,15] Furthermore, elevated CECs in cancer patients were found to be nearly normalized when the tumor was removed surgically or with chemotherapy.[15] Therefore, most CECs are considered to be disseminated tissue endothelial cells in the tumors and the CEC number may reflect the extent of tumor angiogenesis. Indeed, the CEC level has been demonstrated to correlate with the plasma level of VEGF, one of the pivotal factors promoting tumor angiogenesis.[15] Mancuso et al. reported that CEC kinetics and viability are promising predictors of the response to chemotherapy with antiangiogenic activity in patients with advanced breast cancer.[16] Thus, CEC is likely to be a useful marker for predicting the effectiveness of chemotherapy as a noninvasive angiogenesis marker.

NSCLC is the leading cause of cancer-related death worldwide. NSCLC accounts for approximately 50% of patients presenting with unresectable advanced stage,[17] and platinum-based chemotherapy offers only a small improve-

*Shien-Lab; †Medical Oncology, National Cancer Center Hospital, Chuo-ku, Tokyo, Japan; ‡Center for Molecular Biology and Cytogenetics, SRL Inc., Shinmachi, Hino-shi, Tokyo; and §Department of Genome Biology, Kinki University School of Medicine, Osaka-Sayama-shi, Osaka, Japan.
Disclosure: The authors declare no conflicts of interest.
Address for correspondence: Fumiaki Koizumi, MD, PhD, Shien-Lab, National Cancer Center Hospital, 5-1-1 Tsukiji, Chuo-ku, Tokyo, Japan. E-mail: fkoizumi@gan2.res.ncc.go.jp
Copyright © 2009 by the International Association for the Study of Lung Cancer
ISSN: 1556-0864/09/0402-0208

Copyright © 2009 by International Association for the Study of Lung Cancer

ment in survival with advanced NSCLC.[18,19] Over the past decade, several new agents against NSCLC have become available, including the taxanes, gemcitabine, vinorelbine, and irinotecan. The combination of platinum and these new agents has resulted in a high response rate and prolonged survival compared with older chemotherapy regimens (e.g., vindesine, mitomycin, ifosfamide, with cisplatin). Therefore, these regimens are considered standard chemotherapy for advanced NSCLC.[20–26] Although new agents have different mechanisms of action, these combination regimens have not been administered based on the biologic characteristics of each tumor.

Paclitaxel inhibits several endothelial cell functions in vitro such as proliferation, migration, morphogenesis, and metalloprotease production.[27–29] These activities result in antiangiogenic activity in in vivo xenograft models.[27,30] Interestingly, human endothelial cells are more sensitive to paclitaxel than other cellular types.[29] We hypothesized that the CEC value is associated with tumor neovascularization, which is one of the targets of paclitaxel. In the present study, we investigated whether the CEC count at baseline is associated with the effectiveness of the CDDP plus paclitaxel regimen in patients with advanced-stage NSCLC.

MATERIALS AND METHODS

Patients

Patients with histologically or cytologically documented advanced NSCLC were eligible for this study. Each patient was required to meet the following criteria: (1) no prior treatment including chemotherapy, surgery, irradiation, or any fluid drainage; (2) no prior general anesthesia for diagnostic procedures including mediastinoscopy or thoracoscopy; (3) no concomitant diseases including ischemic heart diseases, systemic vasculitis, pulmonary hypertension, or serious complications including infectious disease or diabetes; (4) written informed consent. The trial document was approved by the institutional review board. The clinical characteristics of the patients are shown in Table 1.

TABLE 1. Baseline Characteristics of the Patients

Characteristic	$N = 31$ No. (%)
Gender	
Male	17 (55)
Female	14 (45)
Median age (yr)	60
Range	43–71
ECOG performance status	
0	18 (58)
1	13 (42)
Stage	
IIIA	2 (6)
IIIB	7 (23)
IV	22 (71)
Histology	
Adenocarcinoma	23 (74)
Squamous cell carcinoma	4 (13)
Others	4 (13)

Treatment Schedule and Response Evaluation

All patients were treated according to the following chemotherapeutic regimen: paclitaxel at 200 mg/m^2 over a 3-hour period followed by carboplatin at a dose with an area under the curve of 6 on day 1, repeated every 3 weeks. The treatment was repeated for three or more cycles unless the patients met the criteria for progressive disease (PD) or experienced unacceptable toxicity.

The major axis (a) and minor axis (b) of the tumor mass in each patient were measured with computed tomography. Estimated tumor volume (ETV) was calculated using the following formula; ETV = $4/3 \times \pi$ (a/2 × b/2) × (a/2 + b/2)/2. Computed tomography examinations were performed before treatment and with every one or two cycles of chemotherapy. Response was evaluated according to the RECIST, and tumor markers were excluded from the criteria.[31]

Assay for CEC

Blood samples from NSCLC patients and healthy volunteers were drawn into a 10-ml Cellsave Preservative Tube (Immunicon Corp. Huntingdon Valley, PA) for CEC enumeration. The CEC protocol used was approved by the Institutional Review Board and written informed consent was obtained from each subject. Samples from NSCLC were obtained before (baseline) and 8 and 22 days after starting chemotherapy. Samples were kept at room temperature and processed within 42 hours after collection. All evaluations were performed without knowledge of the clinical status of the patients. The CellTracks system (Immunicon Corp) which consists of CellTracks AutoPrep system and the CellSpotter Analyzer system was used for endothelial cell enumeration.[32,33] In this system, CD146+/DAPI+/CD105-PE+/CD45APC- cells are defined as CECs. Briefly, cells which express CD146 were immunomagnetically captured using ferrofluids coated with CD146 antibodies. The enriched cells were then labeled with the nuclear dye 4V,6-diamidino-2-phenylindole (DAPI), CD105 antibodies conjugated to phycoerythrin (CD105-PE), and the pan-leukocyte antibody CD45 conjugated to allophycocyanin (CD45-APC). In this system, the CD146-enriched, fluorescently labeled cells were identified as CECs when the cells exhibited the DAPI+/CD105+/CD45- phenotype. We performed CEC enumeration twice, using the same sample, and calculated the mean value.

Statistical Analyses

This study was carried out as exploratory research for detecting CECs from NSCLC patients. The number of enrolled patients was therefore not precalculated. Spearman's correlation analysis was performed to investigate the correlation between CEC count and ETV. Between-group comparisons were made using the t test. The association between CEC count and progression free survival (PFS) was estimated using the Kaplan-Meier method. The log-rank test was used to assess the survival difference between strata. Differences were considered statistically significant at $p < 0.05$.

Copyright © 2009 by the International Association for the Study of Lung Cancer

Copyright © 2009 by the International Association for the Study of Lung Cancer

RESULTS

Patient Characteristics

A total of 32 patients were enrolled in the study between August 2005 and March 2006 (Table 1). One patient withdrew consent to participate. Table 1 summarizes the characteristics of the study population. The median age of the patients was 60 years (range, 43–71). The histologic and/or cytologic diagnosis was adenocarcinoma in 23 patients (74.2%), squamous cell carcinoma in 4 (12.9%), and unclassified NSCLC in 4 (12.9%). There were 17 males (54.8%). The clinical stage was IIIA in 2 patients (6.5%), IIIB in 7 (22.6%), and IV in 22 (71.0%).

Ninety-two CEC samples from 31 patients (three samples per patient) were obtained and analyzed. One sample, obtained 22 days after treatment, was not examined because of inadequate collection.

Quantification of CEC

In 31 advanced NSCLC patients, CECs ranged from 32 to 4501 cells/4.0 ml of blood, mean ± SD = 595 ± 832 at baseline. CEC counts were elevated in a large portion of patients with NSCLC as compared with healthy volunteers (n = 53, mean ± SD = 46.2 ± 86.3/4 ml). Case 21 had an exceptionally high CEC count (4501 at baseline). We did not detect a significant correlation between the CEC count and ETV in the 28 assessable patients (p = 0.84, Figure 1). The analysis of CECs during the first course of treatment showed CEC levels to be reduced by CBDCA plus paclitaxel chemotherapy as compared with pretreatment values (176 ± 141 at 8 days and 173 ± 189 at 22 days after treatment) (Figure 2). These reductions were significant (p = 0.011 on day 8 and p = 0.04 on day 22), but there was no significant difference between CEC amounts on day 8 versus day 22 (p = 0.476). There was no difference in the amount of CEC at baseline when patients were subgrouped according to characteristics, such as sex, smoking history, histologic type, and clinical stage. Furthermore, there was no correlation of CEC amounts with the blood examination data (e.g., number of white blood cells, neutrophils, lymphocytes, hemoglobin, platelets, albumin, LDH, CRP, CEA, CYFRA).

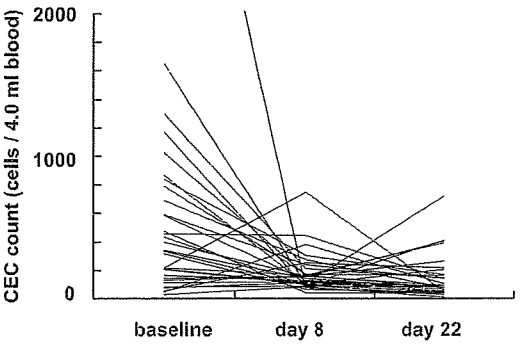

	baseline	day 8	day 22
mean ± SD	595± 832	176± 141 *	173 ± 189 *

FIGURE 2. Circulating endothelial cell (CEC) levels during the first course of CDDP plus paclitaxel chemotherapy. *p < 0.05 versus values at baseline.

CEC Amounts and Objective Tumor Response to Chemotherapy

Thirteen (41.9%) of the 31 patients who received carboplatin and paclitaxel therapy showed a partial response (PR) and 12 (38.7%) showed stable disease (SD). The other 6 patients (19.4%) showed PD. The amounts of CEC at baseline in the patients who showed PR and SD were 516 ± 458/4 ml and 871 ± 1215/4 ml, respectively, and these values were significantly higher than in PD patients (211 ± 150/4 ml, p = 0.023 and p = 0.044, respectively) (Figure 3*A*). Although CEC decrements during chemotherapy were observed in all three subgroups, the extent of the decrements tended to be greater in

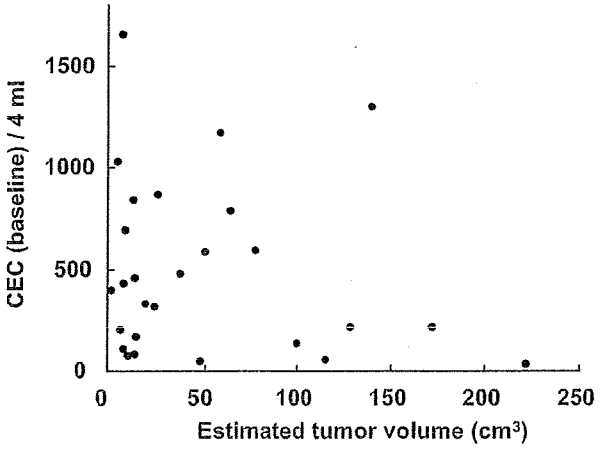

FIGURE 1. Scatter plot analysis to determine the correlation between the number of circulating endothelial cell (CEC) and estimated tumor volume (ETV). ETV is calculated with computed tomography (CT) examination. Case 21 is not included.

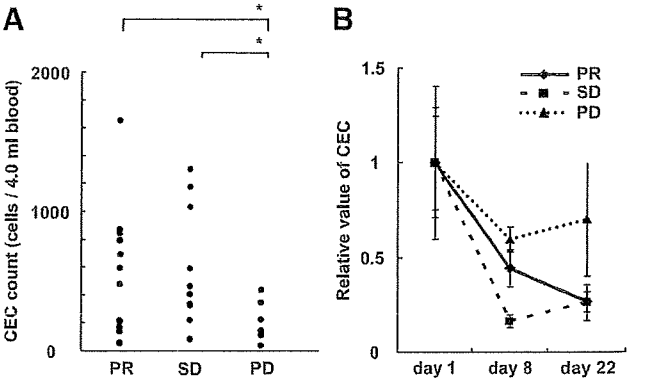

FIGURE 3. *A*, Comparison of circulating endothelial cell (CEC) amount at baseline in non-small cell lung cancer (NSCLC) patients with different clinical responses to CBDCA plus paclitaxel chemotherapy. *p < 0.05 versus values of patients with progressive disease (PD). Case 21 is not included. *B*, Relative change in CEC amount in patients with partial response (PR), stable disease (SD), and PD.

Copyright © 2009 by the International Association for the Study of Lung Cancer

Copyright © 2009 International Association for the Study of Lung Cancer

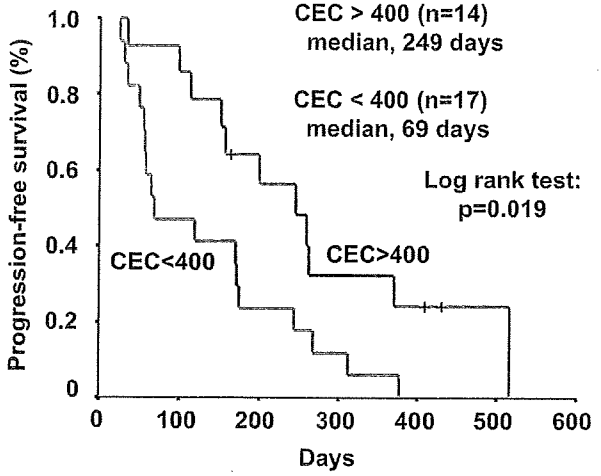

FIGURE 4. Progression-free-survival according to circulating endothelial cell (CEC) count at baseline. The median duration of progression-free survival was greater in patients whose CEC count exceeded 400 (median, 244 days) than in patients whose CEC count was less than 400 (69 days).

patients with PR and SD than in those with PD (Figure 3*B*). In the subgroup analysis, a significant decrease in CECs was observed on day 22 only in PR patients ($p = 0.018$).

CEC Amounts and PFS

For all 31 patients, the median PFS was 154 days (range, 81–361 days). Univariate analysis indicated that patients who had a CEC count of more than 400/4 ml at baseline showed a significantly improved PFS ($n = 14$, median; 244 days) (Log-rank test, $p = 0.019$, Figure 4). A CEC count below 400 at baseline was associated with a poorer PFS ($n = 17$, median; 69 days). The CEC count did not exceed the value of 400/4 ml in any of the healthy volunteers. When we compared the patients whose CEC counts exceeded 200 with those whose counts were less than 200, a consistent difference in PFS was observed between the two groups (>200; $n = 22$, median 227, <200; $n = 9$, median 116, $p < 0.039$).

DISCUSSION

In the present study, we investigated the number of CEC during the first course of CBDCA plus paclitaxel chemotherapy. To our knowledge, this is the first report of CEC in NSCLC patients before treatment. Our findings demonstrated CEC counts in advanced NSCLC at baseline level to be much higher than those in healthy subjects (595 ± 832/4.0 ml versus 32.6 ± 29.5/4.0 ml). Because the NSCLC patients had not yet received anticancer therapy, these increased CECs are likely to be mostly derived from the tumor site. In a previous study, it was found that the amounts of CECs correlate strongly with tumor volume in vivo in an animal model[34]. Nevertheless, we did not find a significant correlation between CECs and ETV. Because the number of CECs could be influenced by many factors related to tumor vasculature, neovascularization, and localization of the tumor, our failure to identify a strong correlation in this study is not surprising. We were also unable to detect a significant direct correlation between CEC amounts and various blood examination data including tumor markers such as CEA and CYFRA. It is unclear at present what biologic characteristics of the tumor or clinical features the CEC number most closely reflects as a biomarker. Mancuso et al. reported that CECs are strongly associated with plasma levels of VCAM-1 and VEGF in breast cancer and lymphoma patients.[15,34] Because VCAM-1 and VEGF are crucial factors for tumor angiogenesis, the variability in CEC values among NSCLC patients might indicate a difference in the neovascularization of each tumor.

We were further able to demonstrate that elevated CECs decreased dramatically after CBDCA plus paclitaxel treatment, but did not reach the level of healthy subjects. Decreased CEC values did not rise again during the first cycle of chemotherapy. Although myelosupression was observed on day 8 and recovered on day 22 in many patients (data not shown), CEC kinetics do not parallel those of WBC, indicating that CEC kinetics might not be influenced by myelopoiesis. Several clinical studies in the field measuring CEC found chemotherapy to be associated with either an increase or a decrease in CECs.[35–39] The different tumor types, stages, prior therapy or not, the anticancer drugs used, measuring points and quantification methods of CEC might have influenced the CEC results after treatment. In the present study, the pretreatment CEC value was much higher than that in lung cancer with metastasis (mean ± SD = 146 ± 270/4 ml), as reported elsewhere.[33] Although the details of the prior therapy in patients with metastatic carcinoma were not provided,[33] chemotherapy can eventually decrease the CEC count.

Schiller et al. compared four standard chemotherapy regimens, cisplatin plus paclitaxel, cisplatin plus gemcitabine, cisplatin plus docetaxel, and carboplatin plus paclitaxel and found no significant difference in survival.[25] Despite the different modes of action of each nonplatinum agent against tumors and different biologic characteristics of each tumor, we could not select the regimen based on these characteristics. In our small study, the patients with PR/SD and longer PFS had higher baseline CEC values. Therefore, it seems that the baseline CEC count is a promising predictor of clinical response to the CBDCA plus paclitaxel regimen and survival in advanced NSCLC. If CEC is a marker for angiogenesis and reflects tumor neovascularization, it is likely that a high CEC is associated with a poor prognosis and lower effectiveness of antiangiogenic therapy. Paclitaxel and docetaxel are categorized as mitotic spindle agents with potent antiangiogenic properties.[27–30] This is why a paclitaxel based regimen might be more effective against tumors with high CEC values. Nevertheless, CEC counts have also been reported to be increased in several clinical syndromes, such as cardiovascular diseases, infectious diseases, and vasculitides.[11–13] The CEC counts in patients with vasculitides have been reported to be dozens of fold higher than those in healthy subjects,[12] therefore, we have to consider the patient condition carefully while interpreting the CEC counts in individual patients, although there were no patients with vasculitis in the present study. Further clinical investigation, with a similar approach, including other nonplatinum anticancer agents, such as

Copyright © 2009 by the International Association for the Study of Lung Cancer

Copyright © 2009 by the International Association for the Study of Lung Cancer

CDDP plus gemcitabine, is essential for the clinical application of CEC for made-to-order chemotherapy in NSCLC.

Antiangiogenic therapy targeting the VEGF pathway such as bevacizumab and VEGFR inhibitors have shown promise in the treatment of solid tumors.[8,39] These agents inhibit endothelial cells through inhibition of the VEGF pathway. It was recently demonstrated that the addition of bevacizumab to CBDCA plus paclitaxel in advanced NSCLC patients produces a significant survival benefit as compared with chemotherapy alone.[40] Considering the outstanding clinical trial and our present study, it would be of great interest to investigate the role of CEC in this regimen.

In conclusion, CECs were measured in NSCLC patients before treatment. Our small clinical study indicates that the CEC count at baseline is a potential biomarker for predicting the response to chemotherapy and PFS, but further clinical evaluation is needed. In the near future, we will start a clinical investigation, using a similar approach, to examine other chemotherapeutic regimens.

ACKNOWLEDGEMENTS

This study was supported in part by a Grant-in-Aid for the 3rd Term Comprehensive 10-year Strategy for Cancer Control from the Ministry of Health, Welfare and Labour, Japan.

REFERENCES

1. Folkman J. Anti-angiogenesis: new concept for therapy of solid tumors. *Ann Surg* 1972;175:409–416.
2. Gasparini G, Harris AL. Clinical importance of the determination of tumor angiogenesis in breast carcinoma: much more than a new prognostic tool. *J Clin Oncol* 1995;13:765–782.
3. Dickinson AJ, Fox SB, Persad RA, Hollyer J, Sibley GN, Harris AL. Quantification of angiogenesis as an independent predictor of prognosis in invasive bladder carcinomas. *Br J Urol* 1994;74:762–766.
4. Takahashi Y, Kitadai Y, Bucana CD, Cleary KR, Ellis LM. Expression of vascular endothelial growth factor and its receptor, KDR, correlates with vascularity, metastasis, and proliferation of human colon cancer. *Cancer Res* 1995;55:3964–3968.
5. Williams JK, Carlson GW, Cohen C, Derose PB, Hunter S, Jurkiewicz MJ. Tumor angiogenesis as a prognostic factor in oral cavity tumors. *Am J Surg* 1994;168:373–380.
6. Koukourakis MI, Giatromanolaki A, Thorpe PE, et al. Vascular endothelial growth factor/KDR activated microvessel density versus CD31 standard microvessel density in non-small cell lung cancer. *Cancer Res* 2000;60:3088–3095.
7. Natsume T, Watanabe J, Koh Y, et al. Antitumor activity of TZT-1027 (Soblidotin) against vascular endothelial growth factor-secreting human lung cancer in vivo. *Cancer Sci* 2003;94:826–833.
8. Hurwitz H, Fehrenbacher L, Novotny W, et al. Bevacizumab plus irinotecan, fluorouracil, and leucovorin for metastatic colorectal cancer. *N Engl J Med* 2004;350:2335–2342.
9. Yang JC, Haworth L, Sherry RM, et al. A randomized trial of bevacizumab, an anti-vascular endothelial growth factor antibody, for metastatic renal cancer. *N Engl J Med* 2003;349:427–434.
10. Johnson DH, Fehrenbacher L, Novotny WF, et al. Randomized phase II trial comparing bevacizumab plus carboplatin and paclitaxel with carboplatin and paclitaxel alone in previously untreated locally advanced or metastatic non-small-cell lung cancer. *J Clin Oncol* 2004;22:2184–191.
11. Mutin M, Canavy I, Blann A, Bory M, Sampol J, Dignat-George F. Direct evidence of endothelial injury in acute myocardial infarction and unstable angina by demonstration of circulating endothelial cells. *Blood* 1999;93:2951–2958.
12. Woywodt A, Streiber F, De Groot K, Regelsberger H, Haller H, Haubitz M. Circulating endothelial cells as markers for ANCA associated small-vessel vasculitis. *Lancet* 2003;361:206–210.
13. Mutunga M, Fulton B, Bullock R, et al. Circulating endothelial cells in patients with septic shock. *Am J Respir Crit Care Med* 2001;163:195–200.
14. Beerepoot LV, Mehra N, Vermaat JS, Zonnenberg BA, Gebbink MF, Voest EE. Increased levels of viable circulating endothelial cells are an indicator of progressive disease in cancer patients. *Ann Oncol* 2004;15:139–145.
15. Mancuso P, Burlini A, Pruneri G, Goldhirsch A, Martinelli G, Bertolini F. Resting and activated endothelial cells are increased in the peripheral blood of cancer patients. *Blood* 2001;97:3658–3661.
16. Mancuso P, Colleoni M, Calleri A, et al. Circulating endothelial-cell kinetics and viability predict survival in breast cancer patients receiving metronomic chemotherapy. *Blood* 2006;108:452–459.
17. Bülzebruck H, Bopp R, Drings P, et al. New aspects in the staging of lung cancer. Prospective validation of the International Union Against Cancer TNM classification. *Cancer* 1992;70:1102–1110.
18. Grilli R, Oxman AD, Julian JA. Chemotherapy for advanced non-small-cell lung cancer: how much benefit is enough? *J Clin Oncol* 1993;11:1866–1872.
19. Non-small Cell Lung Cancer Collaborative Group. Chemotherapy in non-small cell lung cancer: a meta-analysis using updated data on individual patients from 52 randomised clinical trials. *BMJ* 1995;311:899–909.
20. Kubota K, Watanabe K, Kunitoh H, et al. Phase III randomized trial of docetaxel plus cisplatin versus vindesine plus cisplatin in patients with stage IV non-small cell lung cancer: the Japanese Taxotere Lung Cancer Study Group. *J Clin Oncol* 2004;22:254–261.
21. Le Chevalier T, Brisgand D, Douillard JY, et al. Randomized study of vinorelbine and cisplatin versus vindesine and cisplatin versus vinorelbine alone in advanced non-small cell lung cancer: results of a European multicenter trial including 612 patients. *J Clin Oncol* 1994;12:360–367.
22. Belani CP, Lee JS, Socinski MA, et al. Randomized phase III trial comparing cisplatin-etoposide to carboplatin-paclitaxel in advanced or metastatic non-small cell lung cancer. *Ann Oncol* 2005;16:1069–1075.
23. Yana T, Takada M, Origasa H, et al. New chemotherapy agent plus platinum for advanced non-small cell lung cancer: a meta-analysis. *Proc Am Soc Clin Oncol* 2002;21:328a.
24. Baggstrom MQ, Stinchcombe TE, Fried DB, Poole C, Hensing TA, Socinski MA. Third-generation chemotherapy agents in the treatment of advanced non-small cell lung cancer: a meta-analysis. *J Thorac Oncol* 2007;2:845–853.
25. Schiller JH, Harrington D, Belani CP, et al; Eastern Cooperative Oncology Group. Comparison of four chemotherapy regimens for advanced non-small-cell lung cancer. *N Engl J Med* 2002;346:92–98.
26. Ohe Y, Ohashi Y, Kubota K, et al. Randomized phase III study of cisplatin plus irinotecan versus carboplatin plus paclitaxel, cisplatin plus gemcitabine, and cisplatin plus vinorelbine for advanced non-small-cell lung cancer: Four-Arm Cooperative Study in Japan. *Ann Oncol* 2007;18:317–323.
27. Belotti D, Vergani V, Drudis T, et al. The microtubule-affecting drug paclitaxel has antiangiogenic activity. *Clin Cancer Res* 1996;2:1843–1849.
28. Hayot C, Farinelle S, De Decker R, et al. In vitro pharmacological characterizations of the anti-angiogenic and anti-tumor cell migration properties mediated by microtubule-affecting drugs, with special emphasis on the organization of the actin cytoskeleton. *Int J Oncol* 2002;21:417–425.
29. Wang J, Lou P, Lesniewski R, Henkin J. Paclitaxel at ultra low concentrations inhibits angiogenesis without affecting cellular microtubule assembly. *Anticancer Drugs* 2003;14:13–19.
30. Vacca A, Ribatti D, Iurlaro M, et al. Docetaxel versus paclitaxel for antiangiogenesis. *J Hematother Stem Cell Res* 2002;11:103–118.
31. Therasse P, Arbuck SG, Eisenhauer EA, et al. New guidelines to evaluate the response to treatment in solid tumors. European Organization for Research and Treatment of Cancer, National Cancer Institute of the United States, National Cancer Institute of Canada. *J Natl Cancer Inst* 2000;92:205–216.
32. Smirnov DA, Foulk BW, Doyle GV, Connelly MC, Terstappen LW, O'Hara SM. Global gene expression profiling of circulating endothelial cells in patients with metastatic carcinomas. *Cancer Res* 2006;66:2918–2922.
33. Rowand JL, Martin G, Doyle GV, et al. Endothelial cells in peripheral blood of healthy subjects and patients with metastatic carcinomas. *Cytometry A* 2007;71A:105–114.
34. Mancuso P, Calleri A, Cassi C, et al. Circulating endothelial cells as a novel marker of angiogenesis. *Adv Exp Med Biol* 2003;522:83–97.

Copyright © 2009 by the International Association for the Study of Lung Cancer

Copyright © 2009 by the International Association for the Study of Lung Cancer

35. Beaudry P, Force J, Naumov GN, et al. Differential effects of vascular endothelial growth factor receptor-2 inhibitor ZD6474 on circulating endothelial progenitors and mature circulating endothelial cells: implications for use as a surrogate marker of antiangiogenic activity. *Clin Cancer Res* 2005;11:3514–3522.
36. Fürstenberger G, von Moos R, Lucas R, et al. Circulating endothelial cells and angiogenic serum factors during neoadjuvant chemotherapy of primary breast cancer. *Br J Cancer* 2006;94:524–531.
37. Rademaker-Lakhai JM, Beerepoot LV, Mehra N, et al. Phase I pharmacokinetic and pharmacodynamic study of the oral protein kinase C beta-inhibitor enzastaurin in combination with gemcitabine and cisplatin in patients with advanced cancer. *Clin Cancer Res* 2007;13:4474–4481.
38. McAuliffe JC, Trent JC. Biomarkers in gastrointestinal stromal tumor: should we equate blood-based pharmacodynamics with tumor biology and clinical outcomes? *Clin Cancer Res* 2007;13:2643–2650.
39. Hanrahan EO, Heymach JV. Vascular endothelial growth factor receptor tyrosine kinase inhibitors vandetanib (ZD6474) and AZD2171 in lung cancer. *Clin Cancer Res* 2007;13:S4617–S4622.
40. Sandler A, Gray R, Perry MC, et al. Paclitaxel-carboplatin alone or with bevacizumab for non-small-cell lung cancer. *N Engl J Med* 2006;355: 2542–2550; 2007;356:318.

Copyright © 2009 by the International Association for the Study of Lung Cancer

Copyright © 2009 by the International Association for the Study of Lung Cancer

Drug Metab. Pharmacokinet. 24 (1): 118–126 (2009).

SNP Communication

Genetic Variations and Haplotype Structures of the Glutathione *S*-transferase Genes, *GSTT1* and *GSTM1*, in a Japanese Patient Population

Naoko TATEWAKI[1], Keiko MAEKAWA[1,2,*], Noriko KATORI[1,3], Kouichi KUROSE[1,4], Nahoko KANIWA[1,4], Noboru YAMAMOTO[5], Hideo KUNITOH[5], Yuichiro OHE[5], Hiroshi NOKIHARA[5], Ikuo SEKINE[5], Tomohide TAMURA[5], Teruhiko YOSHIDA[6], Nagahiro SAIJO[7], Yoshiro SAITO[1,2] and Jun-ichi SAWADA[1,2]

[1]*Project team for Pharmacogenetics, National Institute of Health Sciences, Tokyo, Japan*
[2]*Division of Functional Biochemistry and Genomics, National Institute of Health Sciences, Tokyo, Japan*
[3]*Division of Drugs, National Institute of Health Sciences, Tokyo, Japan*
[4]*Division of Medicinal Safety Science, National Institute of Health Sciences, Tokyo, Japan*
[5]*Thoracic Oncology Division, National Cancer Center Hospital, National Cancer Center, Tokyo, Japan*
[6]*Genetics Division, National Cancer Center Research Institute, National Cancer Center, Tokyo, Japan*
[7]*Deputy Director, National Cancer Center Hospital East, Kashiwa, Japan*

Full text of this paper is available at http://www.jstage.jst.go.jp/browse/dmpk

Summary: Glutathione *S*-transferases (GSTs) play a vital role in phase II biotransformation of many synthetic chemicals including anticancer drugs. Deletion polymorphisms in *GSTT1* and *GSTM1* are reportedly associated, albeit controversial, with an increased risk in cancer as well as with altered responses to chemotherapeutic drugs. In this study, to elucidate the haplotype structures of *GSTT1* and *GSTM1*, genetic variations were identified in 194 Japanese cancer patients who received platinum-based chemotherapy. Homozygotes for deletion of *GSTT1* (*GSTT1*0/*0* or null) and *GSTM1* (*GSTM1*0/*0* or null) were found in 47.4% and 47.9% of the patients, respectively, while 23.2% of the patients had both *GSTT1* null and *GSTM1* null genotypes. From homozygous (+/+) and heterozygous (*0/+) patients bearing *GSTT1* and *GSTM1* genes, six single nucleotide polymorphisms (SNPs) for *GSTT1* and 23 SNPs for *GSTM1* were identified. A novel SNP in *GSTT1*, 226C>A (Arg76Ser), and the known SNP in *GSTM1*, 519C>G (Asn173Lys, *B), were found at frequencies of 0.003 and 0.077, respectively. Using the detected variations, *GSTT1* and *GSTM1* haplotypes were identified/inferred. Three and six common haplotypes (N≥10) in *GSTT1* and *GSTM1*, respectively, accounted for most (>95%) inferred haplotypes. This information would be useful in pharmacogenomic studies of xenobiotics including anticancer drugs.

Keywords: *GSTT1*; *GSTM1*; nonsynonymous SNP; haplotype; haplotype-tagging SNP

Introduction

Glutathione *S*-transferases (GSTs) (EC 2.5.1.18) are dimeric phase II metabolic enzymes that mainly catalyze conjugation of reduced glutathione (GSH) with a variety of electrophilic compounds including carcinogens, therapeutic drugs and environmental toxins as well as endogenous substances.[1] In addition, GSTs possess selenium-independent GSH peroxidase activity to reduce organic hydroperoxides, and therefore, play significant roles in detoxification, occasionally toxification, and cellular protection against oxidative stress.[2] Noncatalytical-

Received; May 11, 2008, Accepted; August 20, 2008
**To whom correspondence should be addressed:* Keiko MAEKAWA, Ph.D., *Division of Functional Biochemistry and Genomics, National Institute of Health Sciences, 1-18-1 Kamiyoga, Setagaya-ku, Tokyo 158-8501, Japan. Tel. +81-3-3700-9453, Fax. +81-3-5717-3832, E-mail: maekawa@nihs.go.jp*
On April 28th, 2008, the novel variations described in this paper were not found in the Japanese Single Nucleotide Polymorphisms (JSNP) (http://snp.ims.u-tokyo.ac.jp/), dbSNP in the National Center for Biotechnology Information (http://www.ncbi.nlm.nih.gov/SNP/) or SNP500Cancer Database (http://snp500cancer.nci.nih.gov/).
This study was supported in part by the Program for the Promotion of Fundamental Studies in Health Sciences and in part by the Health and Labor Sciences Research Grants from the Ministry of Health, Labor and Welfare.

ly, GSTs modulate signaling pathways by interacting with protein kinases[3] and by binding numerous ligands for nuclear hormone receptors.[4]

Human GSTs are composed of three main families: cytosolic, mitochondrial and microsomal (or membrane-bound). The cytosolic family, which is principally involved in biotransformation of toxic xenobiotics, contains at least 17 genes subdivided into seven separate classes designated alpha, mu, pi, sigma, theta, zeta, and omega.[5,6] Increasing numbers of GST genes are identified as polymorphic.

The θ-class enzyme GSTT1 and the μ-class enzyme GSTM1 exhibit gene deletion polymorphisms (*GSTT1*0* and *GSTM1*0*, respectively).[7] The null genotype of *GSTT1* (*GSTT1*0/*0*) is found in 15–40% of Caucasians and 50–60% of Asians.[7] On the other hand, about half of both Japanese and Caucasians and 30% of Africans are homozygous for the *GSTM1* deletion (*GSTM1*0/*0*).[7] In intact *GSTM1*, alleles **A* and **B* are used to discriminate the single nucleotide polymorphism (SNP) with amino acid substitution (thereafter, nonsynonymous SNP), 519C>G (Asn173Lys) in exon 7, in which both alleles encode proteins that are catalytically identical for the substrates, 1-chloro-2,4-dinitrobenzene (CDNB), *trans*-4-phenyl-3-buten-2-one (tPBO) and 1,2-epoxy-3-(*p*-nitrophenoxy)propane (EPNP).[8] In addition, a tandem duplication in *GSTM1* associated with ultrarapid enzyme activity was observed in Saudi Arabians.[9] A gene-dose effect has been clearly established: that is, homozygously deleted (**0/*0*), heterozygously (**0/+*) and homozygously intact (*+/+*) *GST* genotypes correspond to non-, intermediate, and high conjugators, respectively.[10,11]

A large number of association studies on *GSTM1* and *GSTT1* null genotypes have been performed with inter-individual differences in susceptibility to environmental toxins, cancer and other diseases, and in the outcomes of anticancer treatments. Increased risk of lung, bladder, breast and colon cancers were observed in carriers of *GSTM1* or *GSTT1* null genotypes, while other studies have reported controversial findings.[5-7] As for response to anti-cancer drugs, pharmacodynamic correlations have been investigated, but the obtained results are inconsistent.[6] It should be pointed out that despite the possible gene-dose effect, most association studies were only focused on null genotypes of *GSTM1* and/or *GSTT1*. Therefore, in addition to nonconjugators, discrimination between high and intermediate conjugators would be valuable to evaluate the clinical relevance of these GST loci. Also, certain SNPs in the intact genes might affect either the expression of the gene or the activity of the encoded enzyme.

In this study, we first determined the deletion genotypes (**0/0*, **0/+*, and *+/+*) of *GSTM1* and *GSTT1* by conventional PCR and TaqMan real-time quantitative PCR for 194 Japanese cancer patients treated by platinum-based chemotherapy. Then, we resequenced the homozygous and heterozygous intact *GSTM1* and *GSTT1* genes. Lastly, linkage disequilibrium (LD) and haplotype analyses were performed using the detected SNPs.

Materials and Methods

Human genomic DNA samples: All 194 patients participating in this study were administered carboplatin or nedaplatin in combination with paclitaxel for treatment of various cancers (mainly non-small cell lung cancers) at the National Cancer Center. Genomic DNA was extracted from blood leukocytes from all subjects prior to the chemotherapy. The ethical review boards of the National Cancer Center and National Institute of Health Sciences approved this study. Written informed consent was obtained from all subjects.

Conventional PCR amplification of the *GSTT1* deletion junction: We used the genotyping assay described by Sprenger *et al.*,[10] in which 1460 (for **0* allele) and 466 bp (for exon 5 of the wild-type) PCR fragments were coamplified by multiplex PCR. PCR reactions were performed according to their method with minor modification.[10] Briefly, PCR mixtures contained 100 ng of genomic DNA, 0.2 μM each of the 4 primers reported previously, 0.2 mM each of four deoxynucleotide triphospates (dNTPs), and 0.75 units of HotStarTaq polymerase (Qiagen, Tokyo, Japan) in a 50 μl volume. The PCR conditions were 95°C for 15 min, followed by 30 cycles of 94°C for 30 sec, and 65°C for 1.5 min. PCR fragments were analyzed on 1% agarose gels with ethidium bromide in TAE buffer.

Conventional PCR amplification of *GSTM1*: We used the method of McLellan *et al.* (1997),[9] in which exons 3 to 5 of *GSTM1* were coamplified with β-globin as an internal standard by multiplex PCR. The PCR reactions were carried out according to their method[9] except that 100 ng of genomic DNA and 0.75 units of HotStarTaq polymerase (Qiagen) were used in a 50 μl total volume. The PCR conditions were 94°C for 15 min, followed by 30 cycles of 94°C for 48 sec, 62°C for 48 sec, and 72°C for 1.5 min, and then a final extension for 5 min at 72°C.

Quantitative real-time PCR for *GSTM1* and *GSTT1*: Quantitative real-time PCR using the TaqMan (5′-nuclease) assay system was carried out according to the method of Covault *et al.*,[12] in which the amounts of target *GSTM1* or *GSTT1* were quantified relative to those of the reference β-2-microglobulin (*B2M*) or cannabinoid receptor 1 (*CNR1*), respectively. Briefly, triplicate reactions were performed for 5 ng of genomic DNA used as a template in 1x TaqMan Universal PCR Master Mix with Amp Erase (50 μl) (Applied Biosystems, Foster City, CA, USA). The thermal cycling conditions were 50°C for 2 min and then 95°C for 10 min, followed by 40 cycles of

95°C for 20 sec and 60°C for 1 min with the 7500 Real-Time PCR System (Applied Biosystems).

***GSTT1* DNA sequencing:** The heterozygous and homozygous samples for *GSTT1* (**0/+* and *+/+*), the 5′-flanking region (up to 801 bp upstream from the translation start site), all 5 exons with their surrounding introns and the 3′-flanking region were amplified by PCR and directly sequenced. For the 1st round PCR, the reaction mixtures contained 25 ng of genomic DNA, 1.25 units of Ex-Taq (Takara Bio. Inc. Shiga, Japan), 0.2 mM dNTPs, and 0.2 μM primers listed in **Table 1**. The PCR conditions were 94°C for 5 min, followed by 30 cycles of 94°C for 30 sec, 60°C for 1 min, and 72°C for 2 min; and then a final extension for 7 min at 72°C. The regions from 5′-flanking to exon 1 and from exon 4 to 3′-flanking were amplified separately by the nested PCR with Ex-Taq (1.25 units) and the primer sets (0.2 μM) listed in "2nd round PCR" of **Table 1**. The 2nd round PCR conditions were the same as described in the 1st round PCR. The 2nd round PCR products and the 1st round PCR products for exons 2 and 3 were then treated with a PCR Product Pre-Sequencing Kit (USB Co., Cleveland, OH, USA) and were directly sequenced on both strands using an ABI BigDye Terminator Cycle Sequencing Kit (Applied Biosystems) with the sequencing primers listed in **Table 1** (Sequencing column). Excess dye was removed by a DyeEx96 kit (Qiagen, Hilden, Germany). Eluates were analyzed on an ABI Prism 3730 DNA Analyzer (Applied Biosystems). All novel SNPs were confirmed by repeated sequencing of the PCR products generated by new genomic DNA amplifications. The genomic and cDNA sequences of *GSTT1* obtained from GenBank (NT_011520.11 and NM_000853.1, respectively) were used as reference sequences.

***GSTM1* DNA sequencing:** For samples with **0/+* and *+/+*, genetic variations were identified by resequencing. Particular attention was paid to avoid amplification of sequences of other homologous *GSTMs* because exon 8 of *GSTM1* is 99% identical to that of *GSTM2*.[13] We confirmed that PCR fragments were not amplified from samples with *GSTM1*0/*0* genotypes to evaluate primer specificities. The entire *GSTM1* gene except for the region through exon 8 to the 3′-flanking region was amplified in the 1st round of PCR from 25 ng of genomic DNA utilizing 1.25 units of Ex-Taq with 0.2 μM of primers listed in **Table 2**. Next, three regions (from 5′-flanking to exon 3, from exon 4 to 5, and from exon 6 to 7), were separately amplified in the 2nd round PCR from the 1st round PCR product by Ex-Taq (0.625 units) with 0.2 μM primers listed in **Table 2**. The region from exon 8 to the 3′-flanking was separately amplified from 25 ng of genomic DNA using 0.625 units of Ex-Taq with 0.2 μM primers (listed in **Table 2**). All PCR conditions were the same as those described for *GSTT1*. PCR products were then directly sequenced with the primers listed in

Table 1. *GSTT1* primer sequences

Amplified and sequenced region			Forward primer		Reverse primer		PCR product (bp)
			Sequence (5′ to 3′)	Position[a]	Sequences (5′ to 3′)	Position[a]	
1st round PCR	multiplex	5′-flanking (up to −1366) to exon 1	CACTCCCGCCCCAAATTAGGTT	3776166	ATGATCCCCACCCCTTTATTCG	3774444	1723
		Exon 4 to 3′-flanking region	ATCACAAGGTCAGCAGATTG	3767902	ACTCTTGGCAAACATCAGGG	3766589	1314
		Exon 2	ACATAATCTCTTCTGCAAACTG	3773267	TGTCTCAAGGATACTCTCACCA	3772011	1257
		Exon 3	GCAAATTGTCAGAAAGGTTAAAGA	3770734	CCCACCTCCTGATTAGCTTAGAAG	3768725	2010
2nd round PCR		5′-flanking (up to −801) to exon 1	TTTCAGTGGGATTCGTTTTAGA	3775601	CCCCGTGGTCTATTCCGTGA	3774478	1124
		Exon 4 to 3′-flanking region	CATCACTAATCATTAGGGAA	3767648	CTGGGAAGGGGGTTGTCTTT	3766628	1021
Sequencing		5′-flanking (up to −801)	TTTCAGTGGGATTCGTTTTAGA	3775601	GGCTCGCTCATTTCACTTAG	3775090	
		Exon 1	GGTGGGAAATTCTGACACAC	3775162	CCCCGTGGTCTATTCCGTGA	3774478	
		Exon 2[b]	AAGGGACAAGGTAGTCAGTC	3772758	AACTGGAATAGCAGGAAGGC	3772099	
		Exon 3[b]	AAAAAAAGCGACTATGTATGAAAT	3770153	AGATAAAATGGATGAACAGATGGT	3769662	
		Exon 4	CATCACTAATCATTAGGGAA	3767648	CAGACTGGGGATGGATGGTTGT	3767204	
		Exon 5 to 3′-flanking region	CATCCCCAGTCTGTACCCTTTTCC	3767216	CTGGGAAGGGGGTTGTCTTT	3766628	

[a]The nucleotide position of the 5′ end of each primer on NT_011520.11.
[b]For exons 2 and 3, the 1st round PCR product was directly sequenced.

Table 2. *GSTM1* primer sequences

	Amplified and sequenced region	Forward primer		Reverse primer		PCR product (bp)
		Sequence (5′ to 3′)	Position[a]	Sequences (5′ to 3′)	Position[a]	
1st round PCR	5′-flanking (up to −1309) to exon 7	CCACAAACAAGTTTATTGGGCG	6136872	GTACTAGACATCAATGTCACCGTT	6141347	4476
	Exon 8 to 3′-flanking region	ACAGTGAGATTTTGCTCAGGTATT	6142766	CTCAATTCTAGAAAAGAGCGAG	6145058	2293
2nd round PCR	5′-flanking (up to −650) to exon 3	GACCACATTTCCTTTACTCTGG	6137531	TAAGAATACTGTCACATGAACG	6139231	1701
	Exon 4 to 5	TCTGTGTCCACCTGCATTCGTTCA	6139192	CTGAACACAAACTTTACCATAC	6139883	692
	Exon 6 to 7	CTAATAAATGCTGATGTATCCAAT	6140410	CCTACTATTGCCAGCTCCATCTAT	6141315	906
Sequencing	5′-flanking (up to −650)	GTCCTTCCTATACCACTGACAC	6137567	AACCGAGCAGGGCTCAGAGTAT	6138145	
	Exon 1 to 2	CCCTGACTTCGCTCCCGGAAC	6137956	GGACACCCGTCCCAATTAGACA	6138764	
	Exon 3	TCTGCCCACTCACGCTAAGTTG	6138577	TAAGAATACTGTCACATGAACG	6139231	
	Exon 4 to 5	TCTGTGTCCACCTGCATTCGTTCA	6139192	CTGAACACAAACTTTACCATAC	6139883	
	Exon 6 to 7	CTAATAAATGCTGATGTATCCAAT	6140410	CCTACTATTGCCAGCTCCATCTAT	6141315	
	Exon 8[b]	GAACTTCTGTTTCCCACATGAG	6143164	GAGTAAAGATGGGAATAAACAG	6143735	
	3′-untranslated and flanking region[b]	TCGTTCCTTTCTCCTGTTTATT	6143701	CCTTGGGGTCCTATTCAATGAG	6144362	

[a]The nucleotide position of the 5′ end of each primer on NT_019273.18.
[b]For the region from exon 8 to 3′-flanking, the 1st round PCR product was directly sequenced.

"sequencing" of **Table 2** as described above for *GSTT1*. All novel SNPs were confirmed by repeated sequencing of PCR products that were newly generated by amplification of genomic DNA. The genomic and cDNA sequences of *GSTM1* obtained from GenBank (NT_019273.18 and NM_000561.2, respectively) were used as reference sequences.

Linkage Disequilibrium (LD) and haplotype analyses: Hardy-Weinberg equilibrium and LD analyses were performed by SNPAlyze ver 7.0 (Dynacom Co., Yokohama, Japan). Pairwise LD ($|D'|$ and r^2 values) between two variations was calculated using 102 subjects bearing one or two *GSTT1* genes and 101 subjects bearing one or two *GSTM1* genes. Some haplotypes were unambiguous from subjects with heterozygous **0* alleles. Diplotype configurations were inferred based on estimated haplotype frequencies using Expectation-Maximization algorithms by SNPAlyze software, which can handle multiallelic variations. Haplotypes containing SNPs without any amino acid change were designated as **1*, and nonsynonymous SNP-bearing haplotypes were numerically numbered. Subtypes were named in their frequency order by use of alphabetical small letters.

Results

Determination of deletion polymorphisms in *GSTM1* and *GSTT1*: Both conventional PCR[10] and TaqMan real-time PCR[12] were used to identify deletion of *GSTT1*. By conventional PCR, 92 out of 194 subjects (frequency = 0.474) were assigned as *GSTT1*0/*0*. For all 92 samples with *GSTT1*0/*0*, no significant fluorescence derived from *GSTT1* amplification was detected by TaqMan real-time PCR (mean cycle threshold, Ct, 37.6). Eighty-two (frequency = 0.423) and 20 (frequency = 0.103) subjects were identified as heterozygous (**0/+*) and homozygous (*+/+*) for intact *GSTT1* by conventional PCR, respectively. In the TaqMan real-time PCR, the mean ± SD of relative amounts of *GSTT1* was 1.0 ± 0.111, and 0.448 ± 0.058 for homozygous and heterozygous *GSTT1* carriers, respectively (the mean value for the 20 homozygotes was set as 1). Since the maximum relative amount of *GSTT1* was 1.214, no gene duplication could be inferred for *GSTT1*. The assigned genotypes were consistent between both methods, and their frequencies (**Table 3a**) were in Hardy-Weinberg equilibrium ($p = 0.785$ by Pearson's chi-square test).

As for *GSTM1*, conventional PCR[9] indicated that 93 out of 194 subjects had a homozygous deletion of *GSTM1* (**0/*0*), and that the remaining 101 subjects were either heterozygotes (**0/+*) or homozygotes (*+/+*) for intact *GSTM1*. By real-time PCR, Ct values of 93 samples with the null genotypes were greater than 36.5, which exceeded the sensitivity limits (Ct = 35) of the real-time PCR detection system, indicating that both methods gave consistent results for *GSTM1*0/*0*. As for the 101 subjects with intact *GSTM1* genes (either **0/+* or *+/+*), the distribution of relative amounts of *GSTM1* was clustered into two groups with 1.0 ± 0.083 (16 homozygotes), and 0.51 ± 0.048 (85 heterozygotes) when the mean value of the 16 homozygotes was set as 1. No individuals showed relative amounts more than 1.216, suggesting that the duplication in *GSTM1*[9] was not present in our population. Thus, the frequencies of *GSTM1*0/*0*, **0/+*, and *+/+*, were 0.479, 0.438, and 0.082, respectively (**Table 3a**), and in Hardy-Weinberg equilibrium ($p = 0.576$ by the Pearson's chi-square test).

Table 3b summarizes the results of the distribution of *GSTM1* and *GSTT1* deletions in our Japanese population.

About one-fourth (45 of 194 subjects) were null for both *GSTM1* and *GSTT1* genes.

Variations found in the intact *GSTT1* gene and their LD profiles: Six variations including three novel ones were found by sequencing the 5′-flanking regions, all 5 exons and their flanking regions in the 102 Japanese subjects with **0/+* and *+/+* genotypes (**Table 4**). All detected variations were in Hardy-Weinberg equilibrium ($p \geq 0.44$ by the χ^2 test or Fisher's exact test) when assuming the presence of three alleles (wild, variant and **0* alleles) at each site. One novel nonsynonymous variation, 226C>A (Arg76Ser), was heterozygous in one subject with two intact *GSTT1* genes, and its allele frequency was 0.003 (1/388). The remaining two novel variations in the intronic regions (IVS1+71A>G and IVS2−8A>C) were also rare (allele frequency = 0.003 for both).

Three known variations (IVS1+166A>G, IVS3−36C>T and 824T>C) were found at a relatively high frequency (0.106) and were perfectly linked ($r^2 = 1.0$) with each other.

Variations found in the intact *GSTM1* gene and their LD profile: We found 23 variations, including seven novel ones, in 194 Japanese cancer patients (**Table 5**). Ten variations were located in the 5′-flanking region, 2 in the coding exons, 9 in the introns, and 2 in the 3′-flanking region. All detected variations were in Hardy-Weinberg equilibrium ($p > 0.37$ by the χ^2 test or Fisher's exact test) except for 1107+41C>T in the 3′-flanking region ($p = 0.003$ by the Fisher's exact test). Deviation from Hardy-Weinberg equilibrium for this variation was due to 2 more homozygotes than expected among 16 *GSTM1+/+* subjects.

Seven novel variations, −416G>T and −165A>G in the 5′-flanking region, IVS1+97C>T, IVS1−79G>A, IVS1−78T>A, and IVS2+202G>A in the introns and 1107+128G>A in the 3′-flanking region, were found in single subjects (allele frequencies = 0.003). No novel nonsynonymous SNPs were detected.

Sixteen other variations were already reported or publicized in the dbSNP and/or JSNP databases. They were detected in more than 10 chromosomes (allele frequencies ≥0.026) in our population except for −423C>G and IVS2+118T>C (allele frequency = 0.003).

The pairwise |D′| values between 14 common variations (N≥10) in *GSTM1* were higher than 0.95 except for the combinations between −480A>G and other variations, which showed lower |D′| values ($0.27 < |D'| < 1.0$). As for the r^2 values, strong LDs ($r^2 > 0.87$) were observed among 10 variations,

Table 3. Frequencies of *GSTT1* and *GSTM1* deletions

(a)

	Genotype	N	Frequency (%)	Allele	N	Frequency (%)
GSTT1	**0/*0*	92	0.474	**0*	266	0.686
	**0/+*	82	0.423			
	+/+	20	0.103	+	122	0.314
GSTM1	**0/*0*	93	0.479	**0*	271	0.698
	**0/+*	85	0.438			
	+/+	16	0.082	+	117	0.302

(b)

Genotype combination		N	Frequency (%)
GSTT1	*GSTM1*		
**0/*0*	**0/*0*	45	0.232
	**0/+*	42	0.216
	+/+	5	0.026
**0/+*	**0/*0*	39	0.201
	**0/+*	34	0.175
	+/+	9	0.046
+/+	**0/*0*	9	0.046
	**0/+*	9	0.046
	+/+	2	0.010

**0*, deletion; +, intact gene

Table 4. Summary of *GSTT1* SNPs detected in a Japanese population

SNP ID			Location	Position		Nucleotide change and flanking sequences (5′ to 3′)	Amino acid change	Allele frequency (N=388)
This study	dbSNP (NCBI)	JSNP		NT_011520.11	From the translational initiation site or from the end of nearest exon			
MPJ6_GTT1001[a]			intron1	3774618	IVS1+71A>G	catagcttagggA/Gacttctcccagc		0.003
MPJ6_GTT1002	rs140313	ssj0002194	intron1	3774523	IVS1+166A>G	gatccaagagtcA/Ggggctccccaaa		0.106
MPJ6_GTT1003[a]			intron2	3770088	IVS2-8A>C	catgacccccacA/Ccccacagtgtgg		0.003
MPJ6_GTT1004[a]			Exon3	3770055	226C>A	ctctacctgacgC/Agcaaatataagg	Arg76Ser	0.003
MPJ6_GTT1005	rs140308		intron3	3767603	IVS3-36C>T	ctaactccctacC/Tccagtaactccc		0.106
MPJ6_GTT1006	rs4630	ssj0002197	3′-UTR	3766891	824(*101[b])T>C	ggaatggcttgcT/Ctaagacttgccc		0.106

[a]Novel variations detected in this study.
[b]The nucleotide that follows the translation termination codon TGA is numbered and starts as *1.

Table 5. Summary of *GSTM1* SNPs detected in a Japanese population

SNP ID			Location	Position		Nucleotide change and flanking sequences (5′ to 3′)	Amino acid change	Reported alleles	Allele frequency (N=388)
This study	dbSNP (NCBI)	JSNP		NT_019273.18	From the translational initiation site or from the end of nearest exon				
MPJ6_GTM1001	rs412543	ssj0002146	5′-flanking	6137629	−552C>G	agactaagccct**C/G**ggagtagctttc			0.044
MPJ6_GTM1002	rs3815029	ssj0002147	5′-flanking	6137641	−540C>G	gggagtagctttt**C/G**gatcagaggaa			0.026
MPJ6_GTM1003	rs412302	ssj0002148	5′-flanking	6137701	−480A>G	tcccaggttggg**A/G**ccaccacttttt			0.064
MPJ6_GTM1004	rs3815026		5′-flanking	6137758	−423C>G	cccttgggaact**C/G**gcagcggagag			0.003
MPJ6_GTM1005[a]			5′-flanking	6137765	−416G>T	gaactcggcagc**G/T**gagagaaggctg			0.003
MPJ6_GTM1006	rs4147561	ssj0002149	5′-flanking	6137783	−398C>T	aaggctgaggga**C/T**accgcgggcagg			0.077
MPJ6_GTM1007	rs4147562	ssj0002150	5′-flanking	6137784	−397A>T	aggctgagggac**A/T**ccgcgggcaggg			0.077
MPJ6_GTM1008	rs4147563	ssj0002151	5′-flanking	6137788	−393T>C	tgagggacaccg**T/C**gggcagggagga			0.080
MPJ6_GTM1009	rs28549287	ssj0002152	5′-flanking	6137823	−358G>A	gagctttgctcc**G/A**ttaggatctggc			0.075
MPJ6_GTM1010[a]			5′-flanking	6138016	−165A>G	cttactgagtgc**A/G**gccccaggcgcc			0.003
MPJ6_GTM1011[a]			intron1	6138313	IVS1+97C>T	tcctcttcagggc**C/T**tgcccgcctcag			0.003
MPJ6_GTM1012[a]			intron1	6138398	IVS1−79G>A	ggtacgtgcagt**G/A**taaactgggggc			0.003
MPJ6_GTM1013[a]			intron1	6138399	IVS1−78T>A	gtacgtgcagtg**T/A**aaactgggggct			0.003
MPJ6_GTM1014	rs4147564	ssj0002153	intron2	6138670	IVS2+118T>C	ctgcaggctgtc**T/C**cttccctgagcc			0.003
MPJ6_GTM1015[a]			intron2	6138754	IVS2+202G>A	ctgtctaattgg**G/A**acgggtgtccct			0.003
MPJ6_GTM1016	rs737497	ssj0002154	intron3	6139277	IVS3−78C>T	cccggtctcctc**C/T**ctgctcttgctt			0.077
MPJ6_GTM1017	rs4147565	ssj0002155	intron4	6139462	IVS4+26A>G	gctgcaatgtgt**A/G**gggggaaggtgg			0.080
MPJ6_GTM1018	rs4147566	ssj0002156	intron5	6139772	IVS5+140C>T	cagttattctca**C/T**gactccaatgtc			0.077
MPJ6_GTM1019	rs1065411	ssj0002159	Exon7	6140823	519C>G	atttgagcccaa**C/G**tgcttggacgcc	Asn173Lys	*B	0.077
MPJ6_GTM1020	rs1056806	ssj0002160	Exon7	6140832	528C>T	caagtgcttgga**C/T**gccttcccaaat	Asp176Asp		0.077
MPJ6_GTM1021	rs4147569	ssj0002161	intron7	6143292	IVS7−221G>A	tgtagaatcttc**G/A**taagtgttagct			0.080
MPJ6_GTM1022	rs4147570	ssj0002162	3′-flanking	6144093	1107(*450)+41C>T[b]	ctggccatctac**C/T**cagactgtctgt			0.026
MPJ6_GTM1023[a]			3′-flanking	6144180	1107(*450)+128G>A[b]	ggattctgctgg**G/A**catagtaaggcg			0.003

[a]Novel variations detected in this study.
[b]The position of the 3′ end of exon 8 (1107 or *450)+the position in the 3′-flanking region. (*450 indicates the position from the termination codon TAG.)

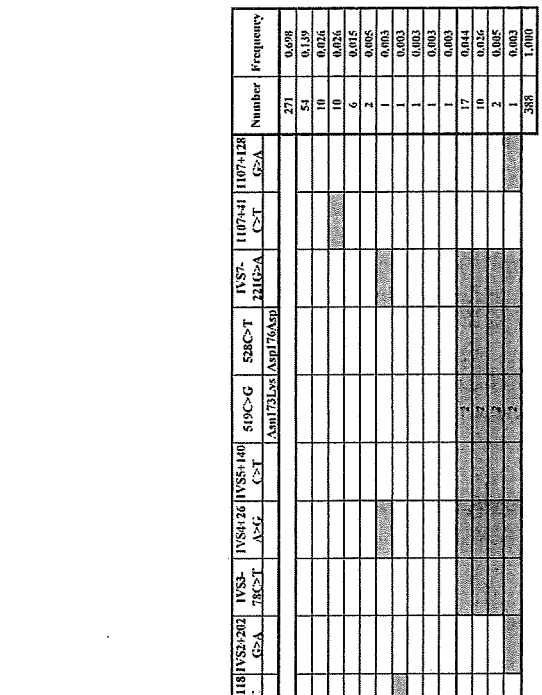

Fig. 1. *GSTT1* (a) and *GSTM1* (b) haplotypes in a Japanese population
Each haplotype is shown in the row, and the alleles are in the columns with the white cell being the major allele and gray cell the minor (nucleotide alteration). §Haplotypes were inferred in only one patient and were ambiguous except for the marker SNPs.

−398C>T, −397A>T, −393T>C, −358G>A, IVS3−78C>T, IVS4+26A>G, IVS5+140C>T, 519C>G (Asn173Lys), 528C>T (Asp176Asp), and IVS7−221G>A. Of these variations, two (−398C>T and −397A>T) and four (IVS3−78C>T, IVS5+140C>T, 519C>G, and 528C>T) pairs of SNPs were in perfect LD ($r^2 = 1.0$).

Haplotype estimation and selection of haplotype-tagging SNPs (htSNPs): Based on results of the LD profiles, haplotypes of *GSTT1* and *GSTM1* were analyzed as one LD block that spans at least 7.7 kb and 6.5 kb, respectively. Using the six variations and null alleles in *GSTT1*, three common haplotypes (*GSTT1*0*, **1a* and **1b*) and three rare haplotypes (**1c*, **1d* and **2a*) were identified or inferred (**Fig. 1a**). Frequencies of the common haplotypes, **0*, **1a*, and **1b*, were 0.686, 0.201, and 0.106, respectively. Thus, the htSNPs are either one of IVS1+166A>G, IVS3−36C>T, and 824T>C for **1b* and 226C>A for **2*.

For the *GSTM1* gene, three groups of haplotypes (*GSTM1*0*, **1* and **2*), each containing 1, 10 and 4 subtypes, were identified or inferred using the 23 variations and the null allele (**Fig. 1b**). The **2* group (**2a* to **2d*) was defined as the haplotypes harboring the known non-synonymous SNP, 519C>G (Asn173Lys), which was previously assigned **B*.[8] The most dominant haplotype was **0* (0.698 frequency), followed by **1a* (0.139), **2a* (0.044), **1b* (0.026), **1c* (0.026), and **2b* (0.026). These six haplotypes accounted for 95% of all haplotypes. The htSNPs that were able to resolve the 5 common haplotypes of the intact genes were −552C>G (**1b* and **1d*), −540C>G (**2b*), −480A>G (**1b* and **2b*), 519C>G (Asn173Lys) (**2*), and 1107+41C>T (**1c*).

Discussion

The present study provides the first comprehensive data on genetic variations of *GSTT1* and *GSTM1* in Japanese, the genes encoding the phase II metabolic enzymes important for cellular defense systems. Moreover, SNPs in intact genes were identified by resequencing, and haplotype structures and tagging SNPs were shown.

It is well recognized that **0* alleles in *GSTT1* and *GSTM1* distribute with different frequencies in several ethnicities. We have shown that 47.4% and 47.9% of our Japanese population homozygously lack *GSTT1* (*GSTT1*0/*0*) and *GSTM1* (*GSTM1*0/*0*), respectively. The *GSTT1*0/*0* frequency is comparable to that reported previously in Japanese (54.0%)[14] and east Asians such as Koreans (46–62%)[7,15] and Chinese (49–58%),[16,17] but was higher than Malay (38%),[17] Indians (16%),[17] Caucasians (15–24%),[7,18] African Americans (22–24%),[7,18] Mexican Americans (10%),[7] and Scandinavians (15%).[7] On the other hand, no marked differences are found in the frequencies of *GSTM1*0/*0* between Caucasians (42–60%)[7,18] and East Asians including Japanese, Koreans

and Chinese (44–63%),[7,14–16] although these frequencies were higher than that of Africans (16–36%).[7,18] The subjects bearing neither *GSTT1* nor *GSTM1* were observed at 23.2%, the frequency of which is similar to Koreans (29.1%)[15] and Shanghai Chinese (24%),[16] but higher than Caucasians (7.5–10.4%)[7,18] and Africans (3.9%).[18]

A number of association studies of the *GSTM1* and *GSTT1* genotypes with cancer susceptibility and cancer therapy outcome have been reported; however, the results are sometimes conflicting.[5–7] In our 194 patients with mainly non-small cell lung cancers, the frequency of *GSTT1*0/*0* and *GSTM1*0/*0* was similar to those in healthy Japanese. This result is in good agreement with a body of literature where the effects of *GSTT1* and *GSTM1* null genotypes on lung cancer development were not clear unless other genetic traits affecting carcinogen metabolism such as *CYP1A1*2A* and *GSTP1*B* (Ile105Val) were combined.[7]

One novel *GSTT1* nonsynonymous variation (226C>A, Arg76Ser) was found in one subject. Arg76 is located in the α3 helix of N-terminal domain I, which forms glutathione binding sites.[19,20] In the crystal structure of human GSTT1-1, this residue closely (2.7 Å) contacts Tyr85 of another subunit (Protein Data Bank, 2C3T).[21] Arg76 is conserved among human, bovine and chicken, whereas this residue is a histidine in mouse and rat. Interestingly, rat and mouse GSTT2 have Ser at position 76.

Of the six SNPs detected in *GSTT1*, three were perfectly linked, resulting in a simple haplotype structure. One of the linked SNPs, 824T>C, was analyzed for various ethnicities in the SNP500Cancer Database (http://snp500cancer.nci.nih.gov/). Its frequency in Japanese (0.106) was comparable to that in Caucasians (0.121), but lower than that in Africans and African-Americans (0.70).

In the *GSTM1* 5′-flanking region (up to −650), eight known SNPs in the NCBI dbSNP database were also detected in this study. This was in contrast to *GSTT1*, in which no SNPs were detected in the 5′-flanking region (up to −801 bp). Murine GSTM1 is transcriptionally upregulated by the Myb proto-oncogene protein through the Myb-binding site (−58 to −63) in the *GSTM1* promoter,[22] whereas no studies on the mechanisms of transcriptional regulation have been performed with human GSTM1. The four common SNPs, −398C>T, −397A>T, −393T>C, and −358G>A (0.075–0.080 in frequencies), were almost perfectly linked with the known SNP, 519C>G (Asn173Lys, *GSTM1*B*) in Japanese. The GSTM1a-1a isozyme (Asn173) and GSTM1b-1b isozyme (Lys173) were reported to have similar catalytic activities *in vitro*.[8] Nevertheless the association of the *GSTM1*A* alleles has been shown with a reduced risk for bladder cancer.[23] Therefore, the functional significance of promoter SNPs on *GSTM1* expression should be further elucidated.

In conclusion, deletions of *GSTT1* and *GSTM1* in Japanese were analyzed by conventional PCR and TaqMan real-time PCR. About one-fourth (0.232 in frequency) of subjects had double *GSTM1* and *GSTT1* null genotypes. In the intact *GSTT1* and *GSTM1* genes, six and 23 SNPs were identified, respectively, and three (*GSTT1*0*, **1a*, **1b*) and six (*GSTM1*0*, **1a*, **2a*, **1b*, **1c* and **2b*) common haplotypes were inferred. Only one rare nonsynonymous SNP (226C>A, Arg76Ser) was found in *GSTT1*, suggesting that this gene is highly conserved. These findings would be useful for pharmacogenetic studies that investigate the relationship between the efficacy of anticancer drugs and *GST* haplotypes.

Acknowledgments: We thank Ms. Chie Sudo for her secretarial assistance.

References

1) Chasseaud, L. F.: The role of glutathione and glutathione *S*-transferases in the metabolism of chemical carcinogens and other electrophilic agents. *Adv. Cancer Res.*, **29**: 175–274 (1979).
2) Hayes, J. D. and McLellan, L. I.: Glutathione and glutathione-dependent enzymes represent a co-ordinately regulated defence against oxidative stress. *Free Radic. Res.*, **31**: 273–300 (1999).
3) Adler, V., Yin, Z., Fuchs, S. Y., Benezra, M., Rosario, L., Tew, K. D., Pincus, M. R., Sardana, M., Henderson, C. J., Wolf, C. R., Davis, R. J. and Ronai, Z.: Regulation of JNK signaling by GSTp. *Embo J.*, **18**: 1321–1334 (1999).
4) Listowsky, I., Abramovitz, M., Homma, H. and Niitsu, Y.: Intracellular binding and transport of hormones and xenobiotics by glutathione-*S*-transferases. *Drug Metab. Rev.*, **19**: 305–318 (1988).
5) Hayes, J. D. and Strange, R. C.: Glutathione S-transferase polymorphisms and their biological consequences. *Pharmacology*, **61**: 154–166 (2000).
6) McIlwain, C. C., Townsend, D. M. and Tew, K. D.: Glutathione *S*-transferase polymorphisms: cancer incidence and therapy. *Oncogene*, **25**: 1639–1648 (2006).
7) Bolt, H. M. and Thier, R.: Relevance of the deletion polymorphisms of the glutathione *S*-transferases GSTT1 and GSTM1 in pharmacology and toxicology. *Curr. Drug. Metab.*, **7**: 613–628 (2006).
8) Widersten, M., Pearson, W. R., Engstrom, A. and Mannervik, B.: Heterologous expression of the allelic variant mu-class glutathione transferases mu and psi. *Biochem. J.*, **276 (Pt 2)**: 519–524 (1991).
9) McLellan, R. A., Oscarson, M., Alexandrie, A. K., Seidegard, J., Evans, D. A., Rannug, A. and Ingelman-Sundberg, M.: Characterization of a human glutathione *S*-transferase mu cluster containing a duplicated GSTM1 gene that causes ultrarapid enzyme activity. *Mol. Pharmacol.*, **52**: 958–965 (1997).
10) Sprenger, R., Schlagenhaufer, R., Kerb, R., Bruhn, C., Brockmoller, J., Roots, I. and Brinkmann, U.: Characterization of the glutathione *S*-transferase GSTT1 deletion: discrimination of all genotypes by polymerase chain reaction indicates a trimodular genotype-phenotype correlation. *Pharmacogenetics*, **10**: 557–

565 (2000).

11) Seidegard, J., Vorachek, W. R., Pero, R. W. and Pearson, W. R.: Hereditary differences in the expression of the human glutathione transferase active on trans-stilbene oxide are due to a gene deletion. *Proc. Natl. Acad. Sci. U S A*, **85**: 7293–7297 (1988).
12) Covault, J., Abreu, C., Kranzler, H. and Oncken, C.: Quantitative real-time PCR for gene dosage determinations in microdeletion genotypes. *Biotechniques*, **35**: 594–596, 598 (2003).
13) Vorachek, W. R., Pearson, W. R. and Rule, G. S.: Cloning, expression, and characterization of a class-mu glutathione transferase from human muscle, the product of the GST4 locus. *Proc. Natl. Acad. Sci. U S A*, **88**: 4443–4447 (1991).
14) Naoe, T., Takeyama, K., Yokozawa, T., Kiyoi, H., Seto, M., Uike, N., Ino, T., Utsunomiya, A., Maruta, A., Jin-nai, I., Kamada, N., Kubota, Y., Nakamura, H., Shimazaki, C., Horiike, S., Kodera, Y., Saito, H., Ueda, R., Wiemels, J. and Ohno, R.: Analysis of genetic polymorphism in NQO1, GST-M1, GST-T1, and CYP3A4 in 469 Japanese patients with therapy-related leukemia/ myelodysplastic syndrome and de novo acute myeloid leukemia. *Clin. Cancer Res.*, **6**: 4091–4095 (2000).
15) Cho, H. J., Lee, S. Y., Ki, C. S. and Kim, J. W.: GSTM1, GSTT1 and GSTP1 polymorphisms in the Korean population. *J. Korean Med. Sci.*, **20**: 1089–1092 (2005).
16) Shen, J., Lin, G., Yuan, W., Tan, J., Bolt, H. M. and Thier, R.: Glutathione transferase T1 and M1 genotype polymorphism in the normal population of Shanghai. *Arch Toxicol*, **72**: 456–458 (1998).
17) Lee, E. J., Wong, J. Y., Yeoh, P. N. and Gong, N. H.: Glutathione *S* transferase-theta (GSTT1) genetic polymorphism among Chinese, Malays and Indians in Singapore. *Pharmacogenetics*, **5**: 332–334 (1995).
18) Chen, C. L., Liu, Q. and Relling, M. V.: Simultaneous characterization of glutathione *S*-transferase M1 and T1 polymorphisms by polymerase chain reaction in American whites and blacks. *Pharmacogenetics*, **6**: 187–191 (1996).
19) Armstrong, R. N.: Structure, catalytic mechanism, and evolution of the glutathione transferases. *Chem. Res. Toxicol.*, **10**: 2–18 (1997).
20) Frova, C.: Glutathione transferases in the genomics era: new insights and perspectives. *Biomol. Eng.*, **23**: 149–169 (2006).
21) Tars, K., Larsson, A. K., Shokeer, A., Olin, B., Mannervik, B. and Kleywegt, G. J.: Structural basis of the suppressed catalytic activity of wild-type human glutathione transferase T1–1 compared to its W234R mutant. *J. Mol. Biol.*, **355**: 96–105 (2006).
22) Bartley, P. A., Keough, R. A., Lutwyche, J. K. and Gonda, T. J.: Regulation of the gene encoding glutathione *S*-transferase M1 (GSTM1) by the Myb oncoprotein. *Oncogene*, **22**: 7570–7575 (2003).
23) Brockmoller, J., Kerb, R., Drakoulis, N., Staffeldt, B. and Roots, I.: Glutathione *S*-transferase M1 and its variants A and B as host factors of bladder cancer susceptibility: a case-control study. *Cancer Res*, **54**: 4103–4111 (1994).